SYNTHESIS OF MULTIWALL CARBON NANOTUBES FROM P-XYLENE AND FERROCENE BY USING VERTICAL CHEMICAL VAPOR DEPOSITION REACTOR FITTED WITH AN ULTRASONIC ATOMIZING HEAD

Fahad Ali Rabbani

DEPARTMENT OF CHEMICAL ENGINEERING

May, 2015

SYNTHESIS OF MULTIWALL CARBON NANOTUBES FROM P-XYLENE AND FERROCENE BY USING VERTICAL CHEMICAL VAPOR DEPOSITION REACTOR FITTED WITH AN ULTRASONIC ATOMIZING HEAD

BY

Fahad Ali Rabbani

A Thesis Presented to the
DEANSHIP OF GRADUATE STUDIES

KING FAHD UNIVERSITY OF PETROLEUM & MINERALS

DHAHRAN, SAUDI ARABIA

In Partial Fulfillment of the
Requirements for the Degree of

MASTER OF SCIENCE

In

CHEMICAL ENGINEERING

May, 2015

KING FAHD UNIVERSITY OF PETROLEUM & MINERALS

DHAHRAN- 31261, SAUDI ARABIA

DEANSHIP OF GRADUATE STUDIES

This thesis, written by Fahad Ali Rabbani under the direction his thesis advisor and approved by his thesis committee, has been presented and accepted by the Dean of Graduate Studies, in partial fulfillment of the requirements for the degree of **MASTER OF SCIENCE IN CHEMICAL ENGINEERING.**

Dr. Zuhair Omar Malaibai
(Advisor)

Dr. Mohammaed Ba-Shammakh

Department Chairman

Dr. Mohammead Mozahar Hossain
(Member)

Dr. Salam A. Zummo
Dean of Graduate Studies

Dr. Basim Abussaud
(Member)

Shaikh Abdur Razzak

Dr. Shaikh Abdur Razzaq
(Member)

1/2/15

Date

Dr. Muataz Ali Atieh
(Member)

Dedicated to all Rabbanies

Especially to My Family and Parents

ACKNOWLEDGMENTS

I wish to express my appreciation to Dr. Zuhair Omer Malaibari who served as my major advisor and kind mentor for kind patience and excellent advices throughout my research work. I would also like to thank to Dr. Muataz Ali Atieh for allowing me to work in his lab and supervising all major and minor issues regarding experimental setup and analyzing results. I pay my gratitude to Dr. Basim Abussaud for help in rigorous analysis of results and valuable comments. I would like to acknowledge Dr. Mohammaead Mozahar Hossain and Dr. Shaikh Abdur Razzak for their technical input and suggestions during my experimental period.

I would also like to thank my parents and family for their support, prayers, inspirations, and encouragement throughout my work. I would also like to thank my friends group: Saqib Javed, Aamir Abbas, Rana Adeem, Waqar Bhatti, Naeem Younas, Farrukh Shahzad. Without my friends it would be a hard journey to complete my stay at KFUPM. I am also thankful to Nano Research Group. Special thanks to Imran Qureshi, Ismael Manasrah, Raja Awais, Sarfraz Muhammad who helped in application and characterization of MWCNT which I synthesized.

I would also like to acknowledge Department of Chemical Engineering for providing an outstanding research environment. I would also like to acknowledge King Fahd University of Petroleum and Minerals for providing a wonderful plateform to complete my graduate studies.

I would like to thank all Pakistani community, all CHE staffs, and technicians for helping during my MS research.

TABLE OF CONTENTS

LIST OF TABLES

LIST OF FIGURES

LIST OF ABBREVIATIONS

AIPO	:	Aluminum isoprop-oxide (Al (OCH (CH_3)$_2$)$_3$)
AO	:	Aluminum oxide (Al_2O_3)
BET	:	Brunauer-Emmett-Teller
CG	:	Carrier gas (Ar)
CNT	:	Carbon nanotubes
CS	:	Catalytic solution (p-xylene and ferrocene)
CVD	:	Chemical vapor deposition
CCVD	:	Catalytic chemical vapor deposition
EDX	:	Energy dispersive X-ray
FCN	:	Ferrocene ($FC_{10}H_{10}$)
IMCNT / IM-CNT	:	Impregnated multiwall carbon nanotubes
IVCVD / IV-CVD	:	Injection vertical chemical vapor deposition
MWCNT / MW-CNT	:	Multiwall carbon nanotubes
pX	:	p-Xylene
RG	:	Reaction gas (H_2)

RS	:	Raman spectra
sccm	:	Standard cubic centimeter per minute
SEM	:	Scanning electron microscope
Slpm or L/m	:	Standard liter per minute
SWCNT	:	Singlewall carbon nanotubes
TEM	:	Transmission electron microscope
XRD	:	X-Ray diffraction

ABSTRACT

Full Name : Fahad Ali Rabbani

Thesis Title : Synthesis of multiwall carbon nanotubes from p-xylene and ferrocene by using vertical chemical vapor deposition reactor fitted with an ultrasonic atomizing head

Major Field : Master in Science of Chemical Engineering

Date of Degree : May, 2015

Chemical vapor deposition (CVD) method has proven its bench marks for the production of different types of carbon nanotubes. In this research CVD reactor is used to produce multiwall carbon nanotubes (MWCNTs) on multi-gram scale by using an improved ultrasonic atomizer as the CVD reactor head for evenly distribution of feed into the reactor. Ferrocene provides catalyst and it is dissolved into p-Xylene which is the carbon source. Pyrolysis of feed solution in the presence of reaction gas (RG), H_2, and carrier gas (CG), Ar, resulted in successful production of MWCNTs. Effect of temperature, feed injection rate, RG flow rate, and reaction time have been investigated in this research. *In situ* impregnation of Al_2O_3 on MWCNT is also carried out by injecting aluminum isopropoxide along with feed solution. The synthesized MWCNT and impregnated multiwall carbon nanotubes (IM-CNT) is characterized by using SEM, TGA, TEM, EDX, BET and XRD. Also; yield, specific heat, viscosity, overall heat coefficient, thermal conductivity of specific samples are calculated. The results obtained indicated that high aspect ratio MWCNT was obtained ranging between 4000-12000. Also a high surface area of 820 m^2/g was noted in case of IMCNT.

ملخص الرسالة

الاسم الكامل: فهد علي رباني

عنوان الرسالة: : تصنيع الأنابيب الكربونية المتناهية الصغر من ال ب-زايلين والفيروسين باستخدام المفاعل العمودي لترسيب الأبخرة الكيميائية والمزود بتقنية رذاذ الموجات الفوق الصوتية.

التخصص: هندسة كيميائية

تاريخ الدرجة العلمية: أيار 2015

إن طريقة ترسيب الأبخرة الكيميائية ومعاييرها تم التثبت من فاعليتها في انتاج الأنواع المتعددة من الأنابيب الكربونية المتناهية الصغر. في هذا البحث تم استخدام طريقة ترسيب الأبخرة الكيميائية في انتاج الأنابيب الكربونية المتناهية الصغر والمتعددة الطبقات وذلك لإنتاج بعض الجرامات من هذا المنتج عن طريق استخدام الأوتومايزر ذو الموجات فوق الصوتيه المحسن كجزء رئيسي في مفاعل ترسيب الأبخرة الكيميائية وذلك لتحسين توزيع التغذية القادمة الى المفاعل. في هذا المفاعل تم استخدام الفيروسين كمحفز للتفاعل وهذا المحفز سيكون ذائبا في الزايلين الذي بدوره يكون مصدر الكربون. أدى الإنحلال الحراري بالإضافة إلى وجود بعض الغازات مثل الغاز الناتج عن التفاعل و الهيدروجين و الأرغون والغاز الناقل إلى تكون الأنابيب الكربونية المتناهية الصغر بنجاح. تم دراسة كثير من العوامل التي ممكن أن تؤثر على إنتاجية الأنابيب المنتهية الصغر مثل تأثير الحرارة وتأثير التغير في معدل التغذية للمفاعل و معدل تدفق الغاز الناتج عن التفاعل و الوقت اللازم للتفاعل. أيضا تم تطعيم سطح الأنابيب الكربونية المتناهية الصغر بأكسيد الأمنيوم في نفس وعاء التفاعل وذلك عن طريق حقن الألمنيوم بروبوكساید متزامنا مع التغذية الواردة الى المفاعل. في هذا البحث أيضا تمت معاينة الأنابيب الكربونية المتناهية الصغر المطعمة وغير المطعمة باستخدام عدة أجهزة وهي مجهر المسح الإلكتروني و تحليل التدهور الحراري و محلل مساحة السطح و تحليل التشتت الطيفي للأشعة إكس و اختبار حيود الأشعة السينية وأيضا باستداخم جهاز المسح الأكتروني المتناهي الأبعاد. بما في ذلك أيضا تم حساب الإنتاجية للعينات و الحرارة النوعية واللزوجة والمعامل الحراري الشامل بالإضافة إلى الموصلية الحرارية. وأخيرا تم استخدام الأنابي الكربونية المصنعة المطعمة وغير المطعمة في تطبيق إزالة المعادن الثقيلة من المياه الملوثة وتمت مقارنة النتائج للأنابيب الكربونية المصنعة بنتائج الأنابيب الكربونية المتناهية الصغر التجارية المطعمة وغير المطعمة أظهرت النتائج التم تم الحصول عليها ارتفاع في نسبة طول الأنبوب الى قطره حيق بلغت هذه النسبة ما قيمته 4000 – 12000 كما لوحظ ارتفاع في مساحة سطح الأنابيب والتي بلغت 820 م^2/غم.

.

CHAPTER 1

INTRODUCTION

In the last decade, enormous study has been done on carbon nanotube (CNT) production. Different routes, for CNT synthesis, and precursor used resulted in variety of carbon nano materials. By tuning reaction dependents, one can produce single wall carbon nanotubes (SWCNTs) or multi wall carbon nanotubes (MWCNTs). Novel properties of CNTs make them unique in different user products, such as, food, clothes, pharmaceuticals, electronics, sensors, purification and cleaning products. A rough forecast declares a trillion-plus investment by 2015 on nanotechnology that will affect global economics. The convenient production and applications of CNTs on a large scale could not be achieved because of the challenges in production, purification, dispersion, and commercial application. This research is a step to meet the challenges for CNT production and to fill the gap linking scientific research and industrial development. Vertical chemical vapor deposition reactor is used, in which concurrent, downstream feed is introduced from top at specific temperature to obtain MWCNTs at bottom. Different parameters, such as, temperature, ratio of catalyst to precursor, flow rate of feed streams, and residence time has been studied for high yield and ultra-pure CNT.

1.1 History & Future of Carbon Nanotube (CNT)

Iijima (1991) used an arc discharge method (ADM) to synthesize carbonaceous group of materials and discovered thin and long carbon straw of nanotubes by using TEM (Iijima, 1991). The length of these carbon nanotubes was varied from several nanometers to micrometers with the diameter range from 2.5 nm to 30 nm. In 1992, Ebbesen and Ajayan observed that the yield of CNTs could be increased exponentially in the chamber of arc by using high pressure (Ebbesen & Ajayan, 1992). In 1993, carbon nanotubes of diameter one nm had been produced using ADM by Bethune and Iijim (Bethune et al., 1993). In 1996, Smalley and his group (lee et al. 1996) used laser vaporizing method (LVM) for graphite and reported only single wall nanotubes with same diameter. These tubes had an affinity to shape associated bundles which drove Smalley to entitle the bundles as 'rope'. Yacamán et al., (1993) used chemical vapor deposition method (CVDM) and made a history in production and implementation of carbon nanotubes (José-Yacamán, Miki-Yoshida, Rendón, & Santiesteban, 1993). From that time, the production and implementation of carbon nanotubes has been studied energetically in the entire world.

Irrespective to observation of hollow carbon nano fibers in 1950s, the industrial scale production of MWCNT started in 1980 following to become a worldwide hot topic for research in the beginning of 1990. But atypical commercial production of MWCNT had been observed in the past decade. Production capacity has amplified 10 times, all over the world since 2006; whereas carbon nanotubes related journal publication and patents are continuously increasing each year (Figure 1.1) (De Volder, Tawfick, Baughman, & Hart, 2013).

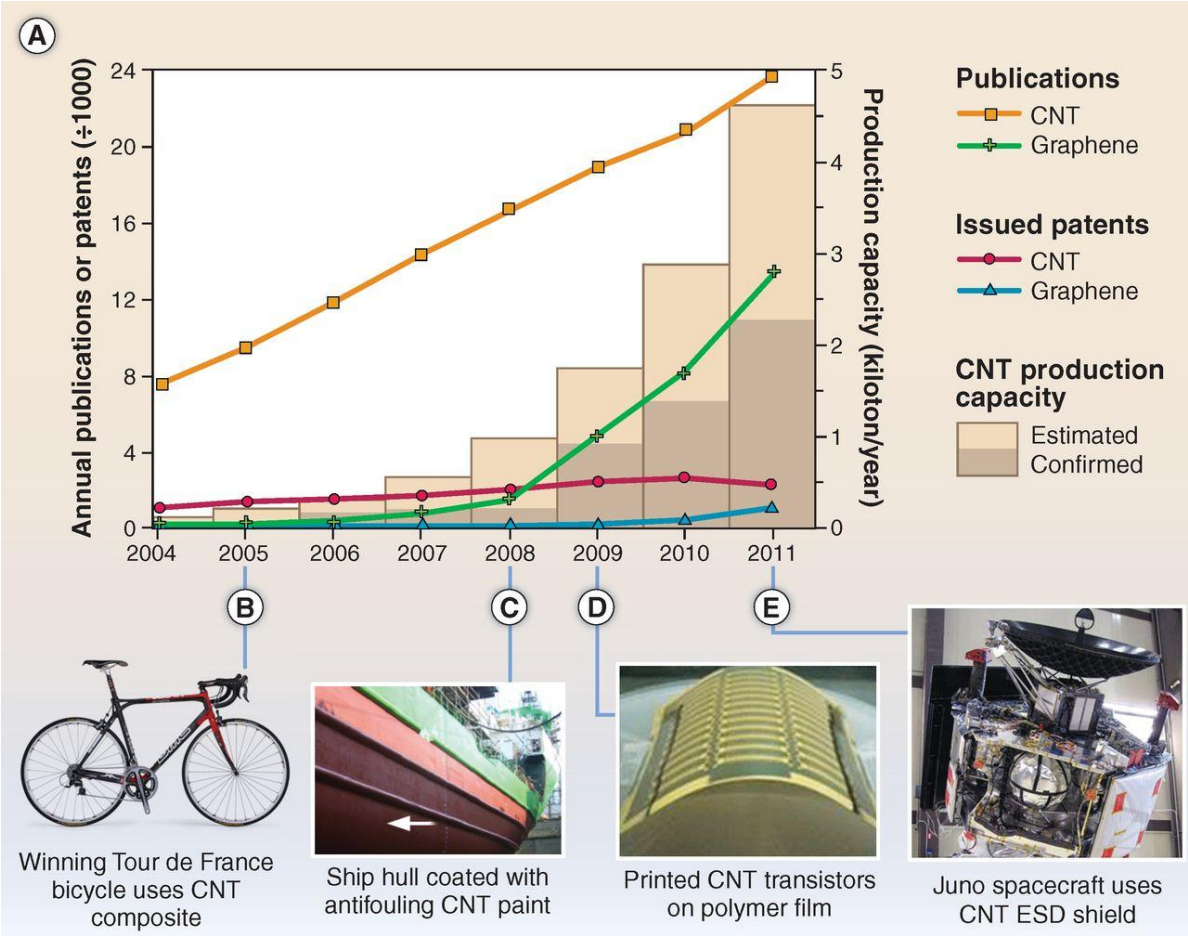

Figure 1.1: Carbon nanotubes in research and commercialization. (A) Annual publications or patents. (B to E) Products related to CNT composites: bicycle frame, antifouling coating, printed electronics, electrostatic discharge shielding.

1.2 Objectives of Research

1.2.1 Main Objective

The main objective of this research is to investigate the production of multiwall carbon nanotubes from p-Xylene and Ferrocene by using vertical chemical vapor deposition reactor fitted with an ultrasonic atomizing head.

1.2.2 Sub Objectives

This main objective could be followed by the following steps:

1- Fabrication of injected vertical CVD reactor with an improved atomizing injection head.

2- Optimization of reaction parameters, such as: temperature, reaction time, feed injection rate, and gases flow rates, to improve the properties of the produced CNTs.

3- Impregnation of Al_2O_3 on MWCNT by using Aluminum Isopropoxide and optimization of impregnation parameters.

4- Characterization of both types of synthesized CNTs by SEM, EDX, TGA, TEM and BET to investigate the effect of varying the parameters in step 2 and 3.

CHAPTER 2

LITERATURE REVIEW

These days nanostructure materials have turned into the essential exploration bearing; for such a variety of fields like science, electronic gadgets, and mechanical and field outflow properties. The late applications of carbon nanotube and carbon nanofiber are: extreme support filaments for composites (high quality, high angle proportion, high thermal and chemical soundness); directing materials as nanowires; field emitters (individual nanotube field emitters, extensive range level board shows); nanotools (tips for Scanning Tunneling, Atomic Force, Magnetic Resonance and Chemical/Biological Force Microscope tips), nano controllers and nanotweezers (Dresselhaus, 1998).. Figure 2.1 shows the structure of various carbonaceous materials.

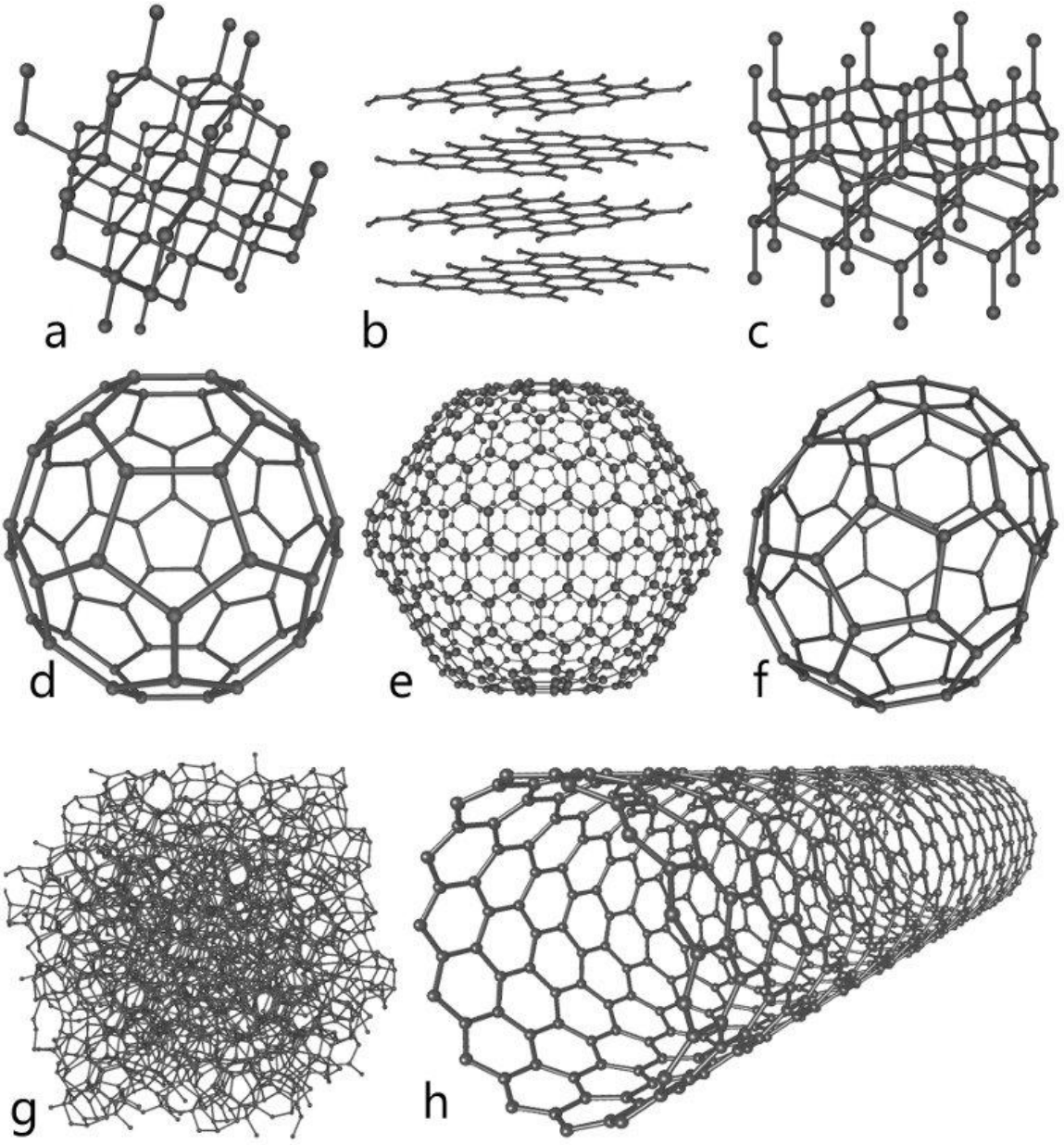

Figure 2.1: The structure of eight allotrops of carbon: a) Diamond b) Graphite c) Lonsdaleite d) C60 (Buckminster fullerene) e) C540 Fullerene f) C70 Fullerene g) Amorphous carbon h) Single-walled carbon nanotubes(http://www.chemicool .com/elements/carbon.html)

2.1 Properties of Carbon Nanotubes

Carbon nanotubes can be classified into three categories on the basis of graphite sheet rolled up structure (Figure 2.2). These types are: Chiral, zigzag, and armchair. Chirality vector (n, m), defines the metallic properties of CNT, and if its value is multiple of 3 then the CNT has metallic properties otherwise it will be a semiconductor nanotube. Whereas, to produce electronic equipment, CNTs with different chiralities can be coupled by hetrojunctions (Dresselhaus, 1998).

CNTs have also unique mechanical properties. They are extremely lightweight composite compound with highly elastic properties. Their high aspect ratio has broadened the application door for nanotubes from field-emission displays to scanning probe microscopic tips.

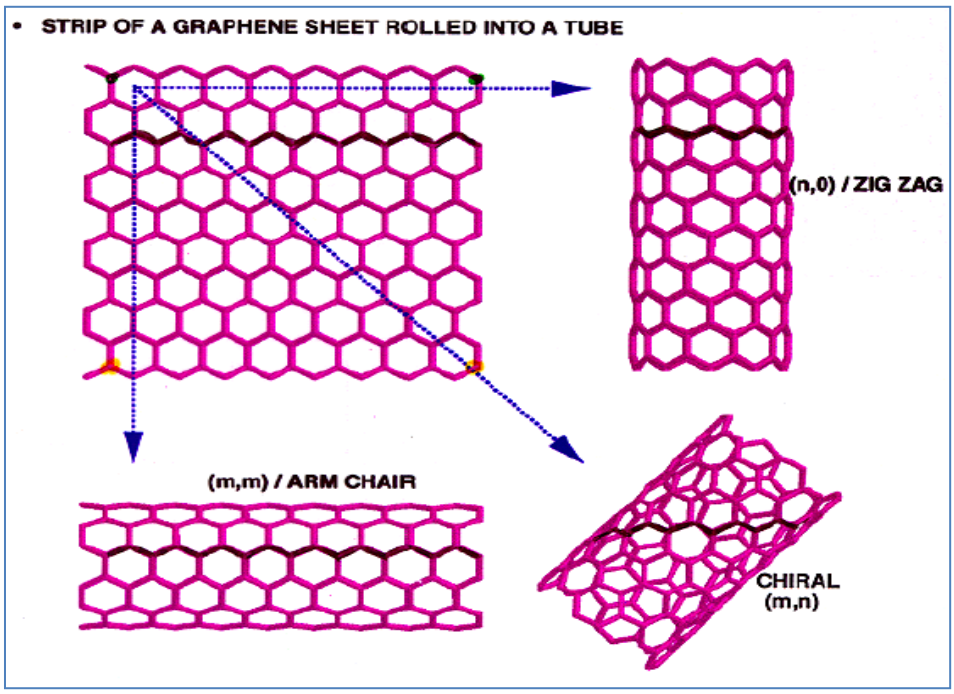

Figure 2.2: Structure of graphite sheet rolled up as CNT (Ajayan, 1999)

2.1.1 Electrical Properties

Carbon nanotubes display diverse electrical properties. Dual nature of metal and semiconductor is one of the central properties of CNT. Scanning tunneling microscopy is the technique by which electronic structure of CNT is characterized. CNT can also be used as a diode (Satishkumar, Thomas, Govindaraj, & Rao, 2000). One can view carbon nanotubes as giant conjugated molecular wires with a conjugation length corresponding to the whole length of the tube (Schujman et al., 2002) and (Collins & Avouris, 2000). Molecular arrangement of CNTs decides the conducting properties resulted from various band composition and band gap. The properties of graphene sheet can be used to find difference in conductivity. When m=n or n-m= 3i, where i is an integer, then CNT shows metallic behavior. Conduction hindrance, when studied by mechanical aspects, appeared to be independent of CNT length (Collins & Avouris, 2000).

2.1.2 Mechanical Properties

CNTs are the best known strongest fiber. Graphite shows the largest basal-plane elastic modulus of any known material. One can see the planer structure of carbon atoms in CNT, in which each carbon atom is chemically bonded with other three carbon atoms and it looks like honeycomb planer structure. These anisotropic properties of CNT make it appropriate for applications in compound materials. CNTs have high Young Modulus and for SWCNT, its value is up to 1 TPa compared to 230 GPa for steel (Schadler, Giannaris, & Ajayan, 1998). Tensile strength of MWCNT was found to be in the range of 1.72 ± 0.64 GPa, by using a tensile tester with very long ropes (~2 mm) (Wagner, Lourie, Feldman, & Tenne, 1998).

2.2 Production Methods of Carbon Nanotubes

Special types of carbon nanotubes, carbon nanofibers, vapor grown carbon fiber and other types of carbon nanostructure materials can be synthesized by different techniques following various routes. Different methods for producing carbon nanotubes (CNTs) and carbon nanofibers (CNFs) are discussed briefly in this section. The most common techniques used nowadays are: arc discharge, laser ablation, and chemical vapour deposition. Cost-effectively reasonable major production and decontamination techniques still have to be developed.

2.2.1 Arc Discharge

Sumio Iijima (1991) discovered this method accidently and now it is used to produce carbon nanotubes on large scale. In this technique an electric direct current (DC) arc is directed towards electrodes which produce high temperature in the chamber (Iijima, 1991). Iijima was the first who observed CNT formation during the fullerenes resulted from arc-discharge method.

In the arc discharge, a vapor is created by an arc discharge between two carbon electrodes with or without catalyst. The distance between electrodes is kept 1 mm. Inert gas, argon or helium, is introduced into the system to avoid any side reaction. High voltage DC provides required temperature and two electrodes produce plasma by vaporizing carbon (Ebbesen & Ajayan, 1992; Iijima, 1991; Journet & Bernier, 1998; Jung et al., 2003; Kiang, Goddard, Beyers, & Bethune, 1995). Anode of the electrodes is made up from transition metals and carbon. Transition metals (Fe, Co, Ni) act as a catalyst during reaction. Reaction parameters, gas pressure, ratio of carbon/catalyst in anode, flow rate,

are varied to control the yield of CNTs, whereas, the purity of CNT is independent of these parameters. Iijima (1991) and Ching-Hwa et al. (1995) provided the reaction condition for arc discharge: 20 volts, 2000-3000 °C, and 100 amps (Figure 2.3).

Random types of CNTs are produced from this method. Up to 30% yield can be achieved with high impurity. Diameters of SWCNT range from 0.61 nm to 1.4 nm and that for MWCNT is 10 nm. This method is comparatively easy to execute from other methods (Dresselhaus, 1998; Journet & Bernier, 1998).

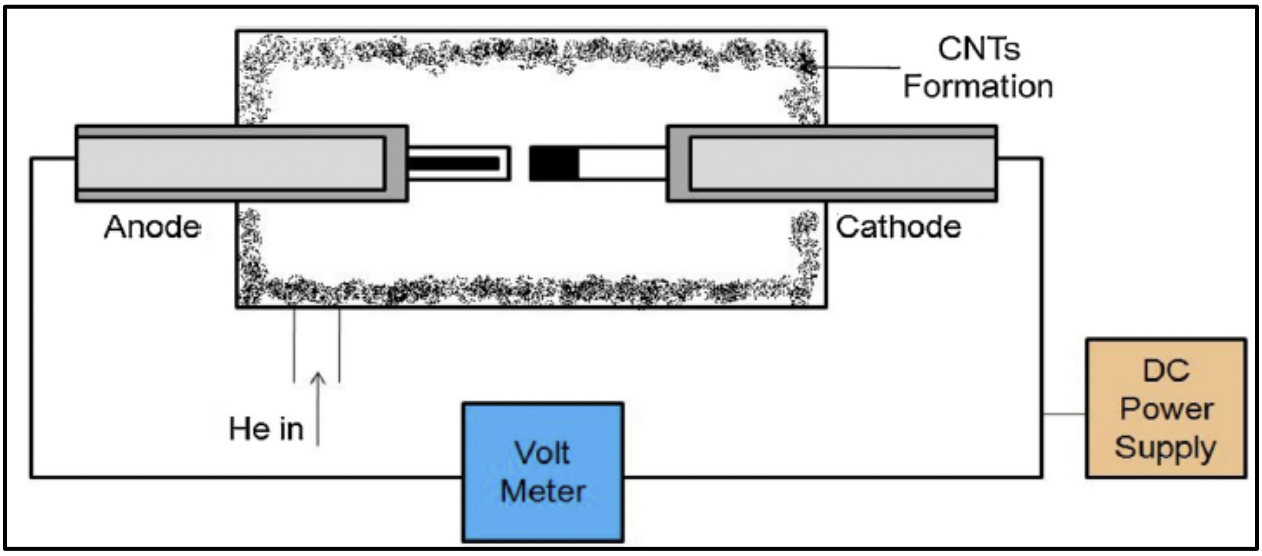

Figure 2.3 Schematic diagram of arc-discharge apparatus (Dresselhaus, 1998)

2.2.2 Laser Ablation

A high intensity laser beam is used in the laser ablation technology, which is directed to a small volume of the target-carbon rod precisely. Meanwhile feedstock gas (CH_4 or CO) is provided to the chamber which contains laser-rod system to enhance the yield. Very small amount of pure CNT can be produced by this method. Smalley's group used laser ablation technique to produce CNT at Rice University (Lee et al. 1996). The apparatus is shown in Figure 2.4.

High Intensity laser beam is directed towards the target metal which is a carbon rod impregnated with transition metal, which acts like catalyst. The laser beam vaporizes the carbon and catalyst from the rod. Furnace is also set into the system to keep constant temperature within the reaction zone. Inert gas (usually argon, Ar) has two functions: First it provides inert medium and second it controls the length of CNT. Therefore, the flow rate of Ar plays an important role for CNT synthesis. After the required time for reaction, argon is purged into the system which takes CNT with it and deposits CNT on the collector.

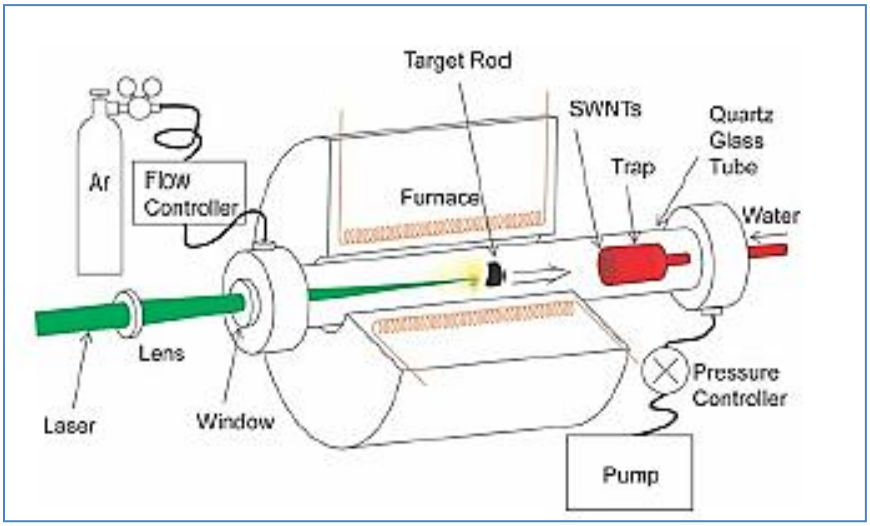

Figure 2.4 Apparatus for laser ablation (Dresselhaus, 1998)

2.2.3 Chemical Vapor Deposition (CVD)

Chemical vapor deposition process can be described as vapors phase deposition of reactant on a heated solid surface where a chemical reaction occurs (Pierson, 1996). Lower hydrocarbons are used in the CVD process, like acetylene (C_2H_2), carbon mono oxide (CO), methane (CH_4), benzene (C_6H_6), and xylene (C_8H_{10}). These hydrocarbons are decomposed by transition metals (Ni, Fe, Co) at high temperatures ranges from 650-1250 ^oC. Initially, this method was used for the production of carbon nanofibers and nanofiber until Yacamán et al. (1993) used CVD method for synthesis of carbon nanotubes (José-Yacamán et al., 1993). CVD reactor usually has two portions, preheating zone and reaction zone, as shown in Figure 2.5.

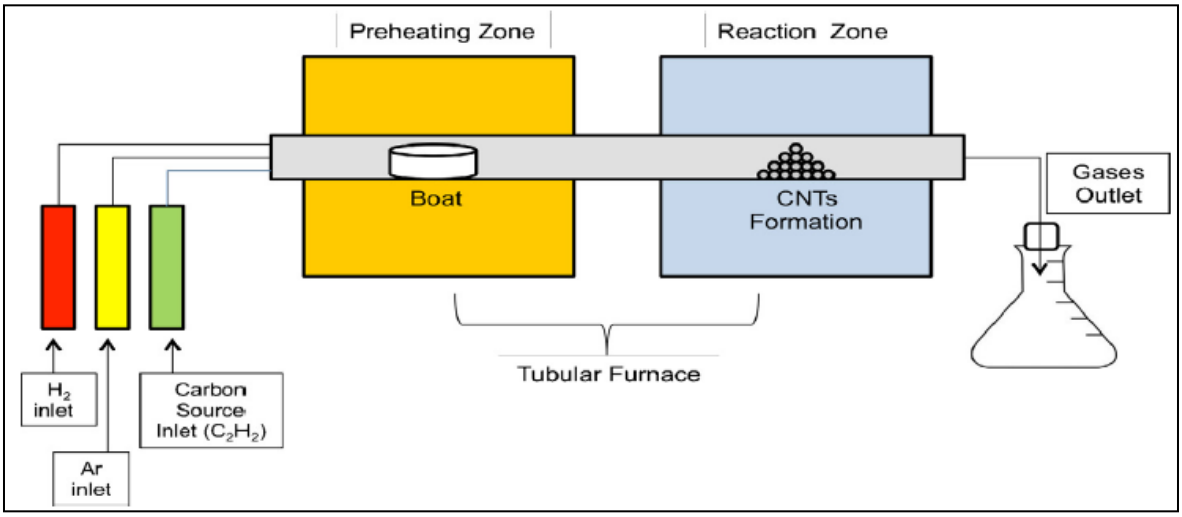

Figure 2.5 Stepwise syntheses of CNT in CVD reactor (Dresselhaus, 1998)

Reaction gases are used to transport reactants from inlet to outlet. Metal catalyst vaporizes in preheating zone and flow through the quartz tube where high temperature is maintained. Then, reaction gases along with hydrocarbon enter in reaction zone where hydrocarbon decomposes onto catalyst surface and starts forming cluster over catalyst surface (Sinnott et al., 1999). After that, external furnace provides required energy to crack the molecule and forms atomic carbon. Later, carbon atoms diffuse over catalyst surface, which is bound to a support, and start forming hollow structure which ends as a carbon nanotube. By using CVD reactor, one can achieve perfect symmetry and control over parameters of reaction which effect the properties of material at nano-scale. Diameter and length of a carbon nanotube can also be controlled. Flexible product can also be synthesized by using proper hydrocarbon /catalyst combination (Hongo, Yudasaka, Ichihashi, Nihey, & Iijima, 2002; X. Q. Wang et al., 2009).

CVD is preferred over other methods due to its highly appreciated features and advantages (Table 2.1). Some of them are described below (Pierson, 1999):

- It is flexible process, easy to handle, and allow different variation in the process.
- It can be used for coating of any type of material.
- Fibers, foams and powders can also be produced by this technique.
- Economically cheap compared to other techniques.

Table 2-1: Comparison of methods for CNT production (Mubarak, Abdullah, Jayakumar, & Sahu, 2014)

Process	**Arc-discharge**	**Laser ablation**	**CVD**
Reaction Temperature	3000-4000 ^{o}C	3000 ^{o}C	500-1100 ^{o}C
Per unit design cost	High	High	Low
Nanotube selectivity	Low	Low	High
Source of carbon	Difficult	Difficult	Easy available
Purification of CNT (high impurities)	High	High	Low
CNT yield	<30 %	~ 70 %	95-99%
Process nature	Batch	Continuous	Continuous
Process parameter control	Difficult	Easy to control	Easy to control
Energy requirement	High	Low	Low
Reactor design	Difficult	Difficult	Easy to design
Nanotube graphitization	High	Middle	Middle

Various techniques have been developed, in past few years, for the production of CNTs by improving some features of CVD reactor (Table 2.2). Some of them are (Dresselhaus, 1998):

I. Vapor phase growth method

II. Substrate / catalyst combination

III. Plasma enhanced process

IV. Fluidized bed CVD

These methods are described in detail in this chapter.

Table 2-2: Comparison of reactor types for CNT production (Su & Chang, 2011)

	Fluidized bed	**Fixed bed**	**Moving bed**	**Transported bed**
Influence on CNT growth	−	− −	− − −	+ + + + +
Heat transfer	+ + + + +	− − −	− − −	−
Mass transfer	+ + + + +	− −	− − − −	+ + +
Flow pattern	well-mixed	piston flow	piston flow	piston flow
Temperature control	+ + + + +	− − − −	− − − −	+ +
Scale-up	+ + + +	− − − −	− − − −	− −
Usable for agglomerated CNTs	+ + + +	+ +	+	−
Usable for aligned CNTs	+	+	− −	+ + +
Achievable capacity	+ + + + +	− − −	− −	+ +
Continuous production	+ + + + +	− − − −	− −	+ +

2.3 Different Routes for CVD Reactors

2.3.1 Vapor Phase Growth Method

Carbon nano materials can also be produced by vapor phase growth mechanism. In this method, a volatile molecule, which should be organanometallic like nichelocene and ferrocene, is introduced into the preheating zone of the reactor where it is vaporized by high temperature and acts as a catalyst. Reaction gases are also supplied directly to the vaporized catalyst where pyrolysis occurs and gas molecules reduce onto catalyst surface forming carbon atoms. This method is usually proposed for CNT and CNF production in mass scale.

This scheme is also known as floating catalyst chemical vapor deposition as catalytic metal and reaction gases are directly supplied into the chamber in the absence of substrate. Vapor phase growth method can be used for synthesis of both, carbon nanotubes and carbon nanofibers.

Figure 2.6 shows a detailed picture of vapor phase growth equipment. Two furnaces are placed around a quartz tube horizontal reactor. First, furnace describes the vaporizing zone, in which low temperature is maintained. Reaction gases are controlled by flow controllers and sent to preheating zone. Powder form catalyst is placed in a ceramic boat from where it vaporizes and moves towards reaction zone, second furnace. High temperature helps pyrolysis of reaction gas in the presence of catalyst. Carbon formed during pyrolysis starts diffusing onto catalyst surface, which results in forming a hollow structure, a CNT (Nikolaev et al., 1999).

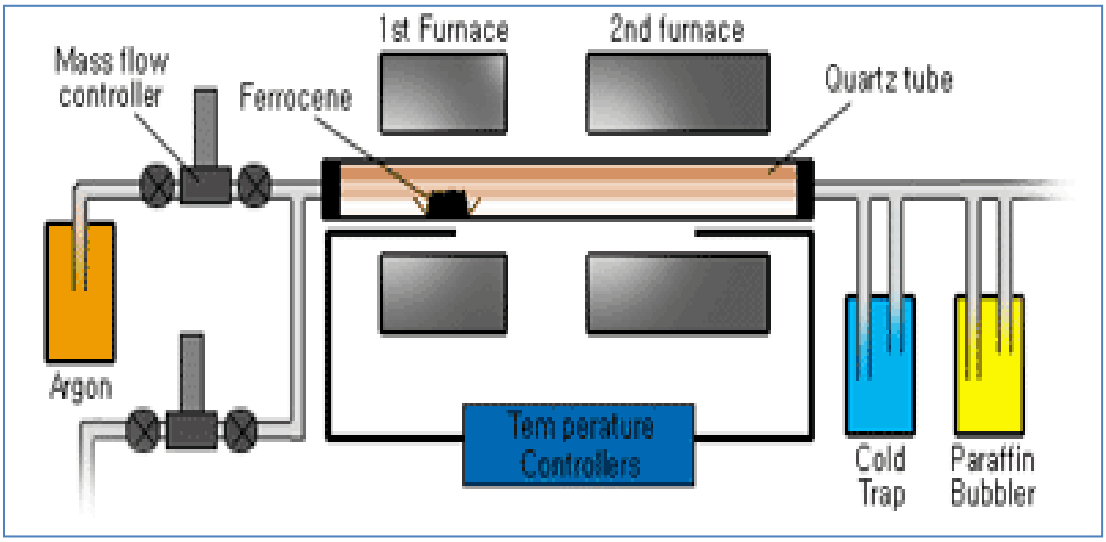

Figure 2.6: Vapor phase growth system (Dresselhaus, 1998)

2.3.2 Substrate Catalyst Method

Different metal and/or metal oxides such as: aluminum dioxide, silicon dioxide, aluminum and silicon are usually used as a substrate for catalyst. First, the transition metal (catalyst) is washed with distilled water and then it is deposited on a substrate. Afterword, the catalyst-substrate compound is kept in a ceramic boat and placed in the middle of CVD furnace (Figure 2.7).

At high temperature, a small layer of catalyst is deposited over substrate and is injected into the reactor along with hydrocarbon precursor. Catalyst breaks hydrocarbon by pyrolysis and results in the formation of CNT. Diameter of CNT is controlled by the thickness of catalyst. Thickness of catalyst is controlled by annealing and its range varies from 1-200 nm (Balogh, Halasi, Korbély, & Hernadi, 2008; Jeong, Olofsson, Falk, & Campbell, 2009; Kong, Soh, Cassell, Quate, & Dai, 1998; Zheng, Li, & Liu, 2002).

Bei and Ping (2005) reported the effect of catalyst/substrate on CNT density and its alignment. They found by changing Ni:Cr ratio and thickness, CNT showed dramatic variation in alignment and thickness (Barreiro et al., 2005). Electron dispersive X-ray (EDX) and high resolution transmission electron scope (HRTEM) results proved that Ni was present in the CNT as catalyst and Cr behaved as a dispersing agent during the reaction. Thus, one can produce aligned CNT for various applications with required diameter by adjusting Ni:Cr thickness and behavior of catalyst.

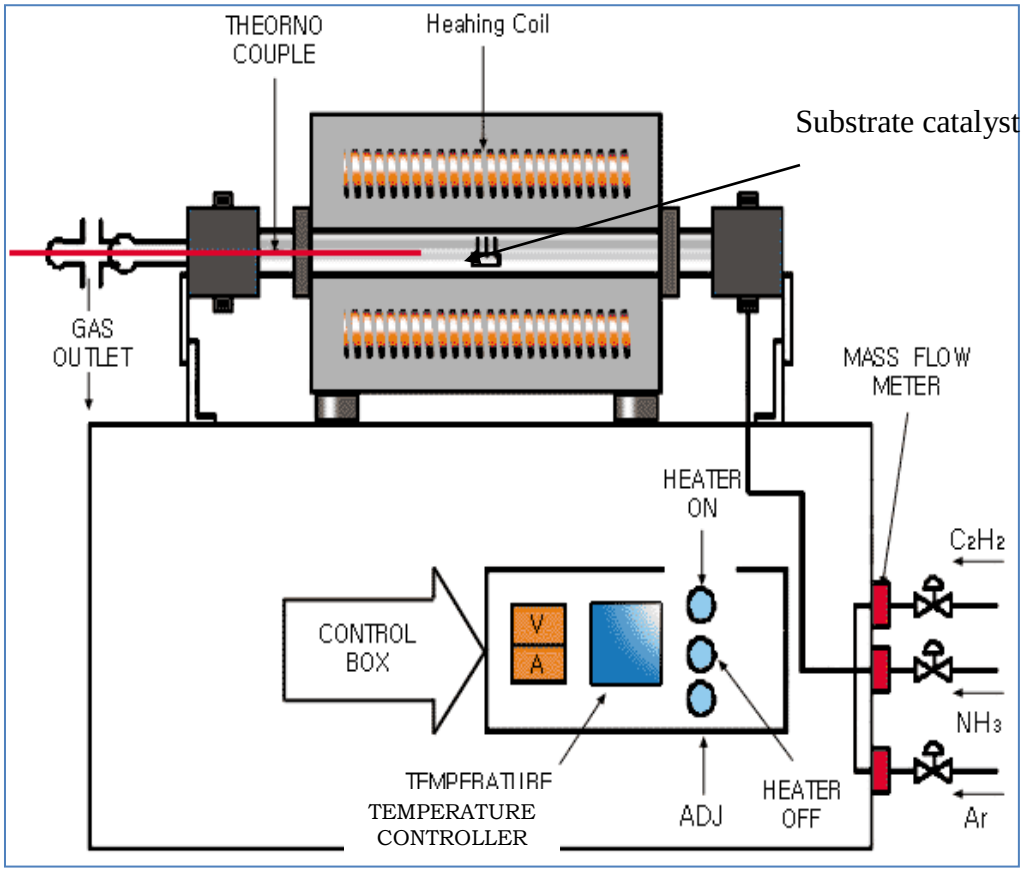

Figure 2.7: Thermal chemical vapor deposition apparatus (Dresselhaus, 1998)

2.3.3 Plasma Enhanced Process

In Plasma enhanced chemical vapor deposition method, catalyst is coated over substrate and CNT produced by this process glows in plasma. Two parallel electrodes are used to produce high intensity plasma. High voltage energy is provided to electrodes by direct current, microwave or radio frequency (Figure 2.8). A substrate is set on the grounded terminal (Dresselhaus, 1998).

Pyrolysis of lower hydrocarbon is difficult to achieve. Therefore high concentration of reducing agent such as H_2, is used to in the reactor system which accelerates pyrolysis of lower hydrocarbons. Sometimes methane (CH_4) and hydrogen (H_2) gases mixture is used in the ratio 1:99 respectively. Temperature of the chamber is kept at 900 °C and pressure varies from 1 to 40 mbar. This method can be used to produce carbon nanotubes and carbon nanofibers (Bower, Zhu, Jin, & Zhou, 2000; T. Ikuno et al., 2002; Takashi Ikuno et al., 2002; Küttel, Groening, Emmenegger, & Schlapbach, 1998; Merkulov, Melechko, Guillorn, Lowndes, & Simpson, 2002; Ren, Zhifeng ; Huang, Zhongping ; J Wang, ui H.; Wang, 2005).

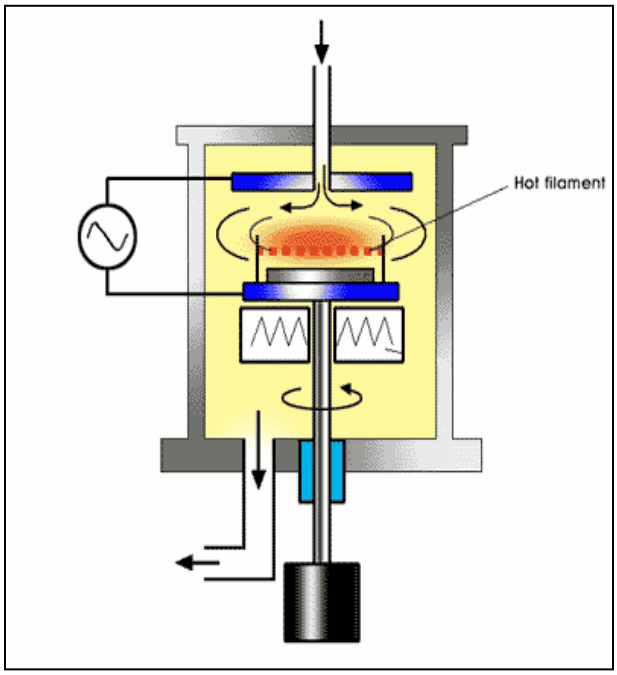

Figure 2.8: Thermal chemical vapor deposition apparatus (Dresselhaus, 1998)

2.3.4 Fluidized-Bed CVD Method

For substantial scale synthesis, the utilization of a fluidized bed reactor has been proposed as an option to avoid deposition of the CNT on fixed bed reactor dividers, however this sort of reactor has not been reported to use it commonly for the production of carbon nanotubes on any scale (Balogh et al., 2008; Perez-Cabero, Rodriguez-Ramos, & Guerrero-Ruiz, 2003; Richter et al., 1996; Venegoni et al., 2002). The setup and a photograph of the framework are demonstrated in Figure 2.9. The reactor is made of a quartz tube with a filter in the center on which the substrate is placed and fluidized by the gas stream in an electrical heater. Besides, the close structure of tube makes it possible to increase contact area of substrate with the gas. After the reaction completion, the Substrate can be removed from the reactor by using suitable solution., the substrate can be uprooted with a sufficient solution (Mauron et al., 2003).

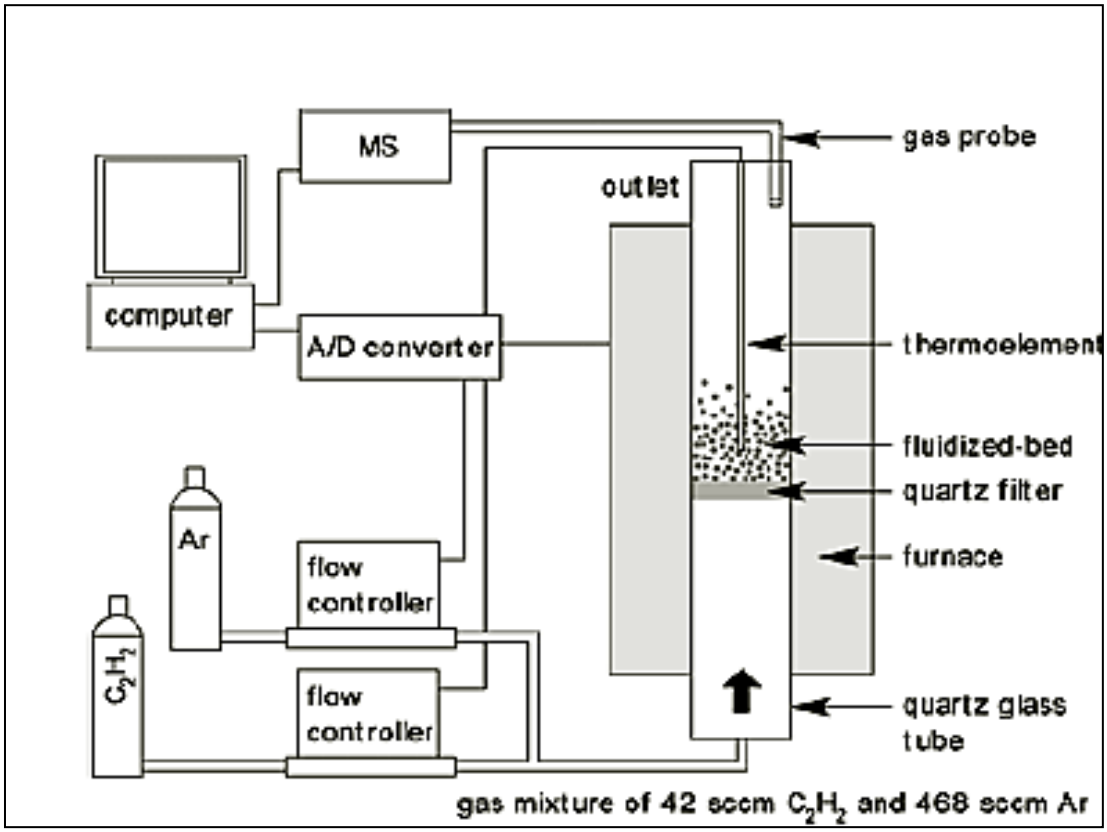

Figure 2.9: Schematic diagram of the fluidized-bed reactor (Dresselhaus, 1998)

2.4 Large Scale Production of Carbon Nanotubes by Using CVD

Cassell et al. (1999) showed an advance method to produce SWCNT on mass scale by using different paths of CVD reactor (Cassell, Raymakers, Kong, & Dai, 1999). By modifying a CVD reactor and using methane as feed, one can produce a large amount of pure CNT by selecting suitable combination of feed and catalyst (Y.-L. Li, Zhang, Zhong, & Windle, 2007). Ratio of catalyst and substrate also effect CNT synthesis process.

Varadan and Xie (2002) used microwave energy in the CVD reactor for synthesis multi wall carbon nanotubes (MWCNTs) on large scale (Varadan & Xie, 2002). The normal diameter of tubes was found to be 20-30 nm. Wang et al. (2002) examined different fluidization characteristics to CNT produced in fluidized-bed reactor (Y. Wang, Wei, Luo, Yu, & Gu, 2002). Carbon nanotubes (CNTs) created by catalytic chemical vapor deposition (CCVD) can be framed into detached agglomerates that can be fluidized along with the synthesis process. This gives an approach to synthesize CNTs on a huge scale, with low cost in a nano-agglomerate fluidized-bed reactor (NAFBR). Charanjeet et al. (2003) reported a unique way to synthesize ultra pure and arranged multi-walled carbon nanotube layers which grew on thin quartz tubes by spurting a mixture of ferrocene and toluene (Öncel & Yürüm, 2006).

Jinyong and Yafei (2006) investigated an easy and new way for large-scale production of arranged carbon nanotubes (CNTs). The product possesses high chemically solubilized and good surface spreading properties at the air/water interface(J. Li & Zhang, 2006). Aurore et al., (2007) studied the catalytic growth of MWCNT and investigated the

reaction parameters: pressure, temperature, residence time and composition of the gaseous segment and synthesized MWCNT on the multi gram level, by using ethylene in fluidized CVD reactor.

2.4.1 Catalyst Effect

For CNT production widely used catalysts which are also most effective are Fe/Co/Ni. Because carbon tendence to dissolve into these metals at high temperature, hence, metal-carbon solution initiate the growth mechanism. (Y. Li et al., 2010) stated that structure of SWCNTs can be controlled by tuning catalysis parameters. Also studied the role of Fe-based nanoparticles, in CVD reactor; for controlling the size of SWCNTs. CNT configuration depends upon the size of catalyst particle as well as on the diffusion rate of carbon into the catalyst. Large particle size of catalyst results low production rate. Whereas the growth rate of CNTs has direct relation to the diffusion rate of carbon into the catalyst (Kim et al., 2003). Other catalysts that are generally used for synthesis of CNT include: cobalt, iron, titanium, nickel, zeolites, and combination of metals and oxides (Mubarak, Abdullah, Jayakumar, & Sahu, 2014).

2.4.2 Substrate Effect

Alumina, silica, quartz, zeolites are extensively used substrate for CNT production catalysts (R. Andrews et al., 1999; Balogh et al., 2008; Jeong et al., 2009; Mamalis, Vogtländer, & Markopoulos, 2004; Merkulov et al., 2002). Substrate has dual effect on catalyst, first it helps to disperse catalyst particle and then it provides support for catalyst which favors the formation of carbon nanotubes. Messina et al., (2008) represented the essential role of precursor and catalyst support in the presence of iron base catalyst to

produce MWCNTs by using CVD (Messina et al., 2008). The results obtained from this study proved different structure and morphology of MWCNT which was produced using ethane and isobutene as precursor gases, and silica and alumina as catalyst substrate.

Craddock & Weisenberger (2014) proposed a method for production of aligned MWCNTs which was substrate free and large sheets. They produced sheets of CNTs on quarts plate with the dimensions ~18 inches long and ~3 inch wide, whereas the height of CNT sheet was ranging from 50 to 250 microns (Craddock & Weisenberger, 2014). However, they used only a small portion of reactor for collection of product. This kind of techniques are good for producing pure-CNT but on the other hand they limits the yield (Rodney Andrews, Jacques, Qian, & Rantell, 2002; Jin, Park, Huh, & Yong, 2001; Kunadian, Andrews, Qian, & Pinar Mengüç, 2009; C. J. Lee, Park, & Yu, 2002; Satishkumar, Govindaraj, & Rao, 1999)To provide maximum area for catalyst to support on, we used quartz tube reactor.

2.4.3 Feed Injection Methods

Fluidized bed reactors are extensively useful for numerous industrial principles, for example special category of chemical reactors, fluid catalytic cracking, fluidized bed combustion, fluidized bed bio-filter or applying a coating on solid items (Vahlas, Caussat, Serp, & Angelopoulos, 2006). One of the main advantages of fluidized bed CVD reactor, other than its commercial use, is that it provides good mixing of catalyst to carbon source. It can bear thermal shocks during exothermic pyrolysis reaction and also it can be scaled up for large production of CNTs. Usually, a horizontal CVD reactor is used for CNT synthesis in which vaporized or gaseous feed enters from one side of the

reactor and effluent leaves from other side. But as an advance method, vertical CVD (VCVD) reactor is also now in practice (Dell'Acqua-Bellavitis, Ballard, Ajayan, & Siegel, 2004; Vahlas et al., 2006; Venegonia, Ph; R, Serp; R, Feurer; Y, 2002). For VCVD reactor, a bed of catalyst with support is prepared for each run. Feed gas is entered from bottom or middle portion of VCVD reactor which fluidize catalyst particle and; CNT forms as a result of thermal cracking in presence of catalyst. Different types of sieves and supports are used to provide good interaction between catalyst and carbon source (Corrias et al., 2003; Morançais et al., 2007; Perez-Cabero et al., 2003; Y. Wang, Wei, Gu, & Yu, 2002; Weizhong et al., 2004). Fluidized velocity is another factor that needs a serious attention to optimize the system.

Muataz et al. (2006), introduced a floating VCVD reactor in which liquid feed is injected from top of the reactor by an injection pump (Muataz, Ahmadun, Guan, Mahdi, & A, 2006). This symmetry of feed injection into the reactor does not involve the calculation of fluidized velocity as fluid enters into the reaction zone of the reactor by inertia and due to gravity effect. Although, vertical CVD reactor was easy to design and operate but due to low surface area of feed particles inside the reactor one can not obtain high yield as compared to that which obtained by horizontal CVD reactor. It is because; liquid feed does not have high surface area which is required for proper conversion of feed into CNT (Ajayan, 1999; Mamalis et al., 2004; Paradise & Goswami, 2007). Also, wide range of diameter of CNTs obtained were obtained because drop size of feed cannot be controlled which effect CNT characterizations. On the other hand, floating VCVD system has advantage over horizontal CVD that it has simple symmetry of reactor, less parameters involvement during reaction and can be used as semi-continue reactor.

On this basis, we made three modifications in floating VCVD reactor by 1) scaling up the reactor, 2) using an ultrasonic atomization system for feed injection, and 3) introducing a collector box in bottom of the reactor. The ultrasonic atomizer was used to increase surface area of feed; as in conventional VCVD reactors, bed of catalyst supported on sieves is used to enhance surface area. So, in this system no need to prepare a bed of catalyst and support before every reaction which is an advantage over VCVD reactors.

There are different types of ultrasonic atomizers which vary in velocity profile, required particle size, heat sensitivity, ultrasonic frequency, dimension (shape and length), and fluid type. Three types of atomizing nozzles are shown in Figure 2.10.

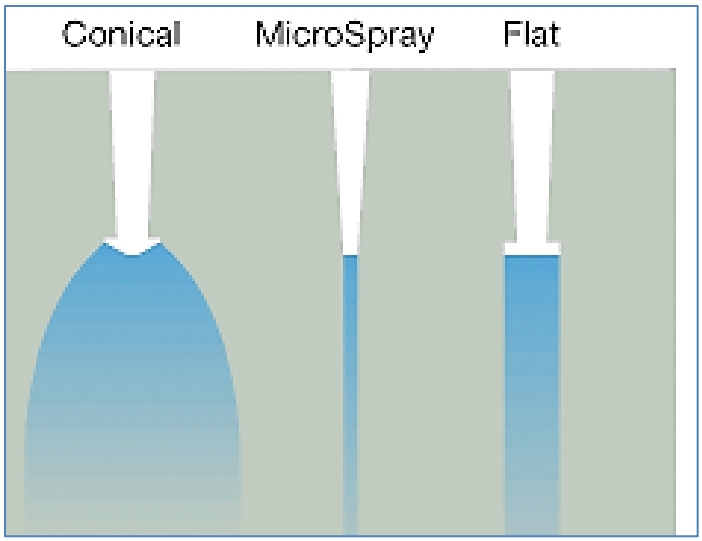

Figure 2.10: Types of Atomizing Nozzles [http://www.sono-tek.com/how-ultrasonic-nozzles-work]

A special conical type of atomizer nozzle was selected which makes an umbrella-shape velocity profile of fluid and hence it distributes liquid feed uniformly into the reactor. This type of IVCVD reactor system had not been used before according to our knowledge. Normally pneumatic pressurized, rotating disc or two feed flow system is used for atomization, which may affect concentration of feed. But, ultrasonic atomizer nozzle consists of two main parts: a transducer; which converts electric signal into frequency, and a nozzle; which shape the velocity profile of fluid (Figure 2.11). Therefore, change in concentration is not possible in this type of atomizer as no moving parts are involved. Reaction gas is also introduced from top head of the reactor which takes atomized feed particles with itself into reaction zone where CNT synthesis starts.

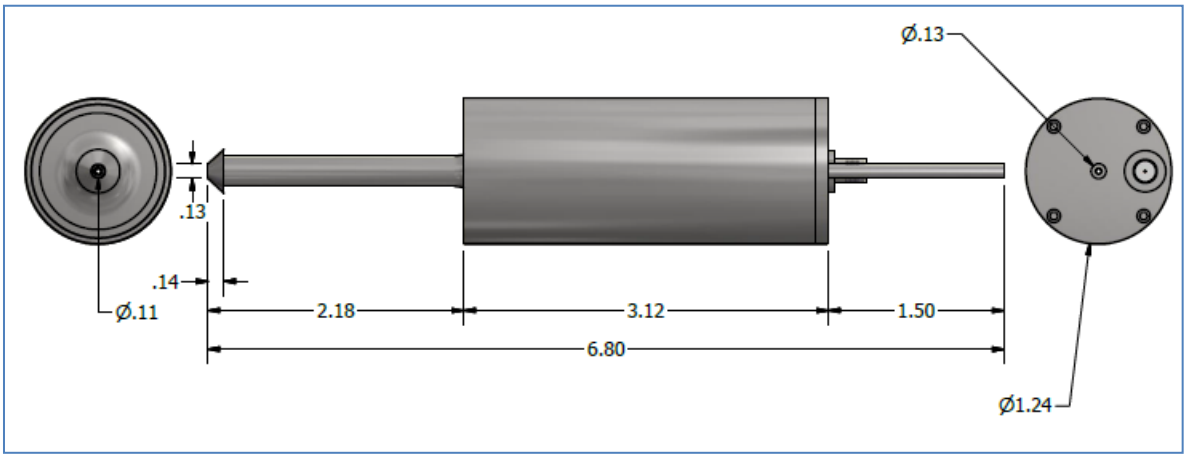

Figure 2.11: Conical Wide Range Atomizing Nozzle (dimensions are in centimeters)

2.5 Impregnation Methods

Iijima reported synthesis of carbon nanotubes for the first time (Iijima, 1991). Till then different routes, precursors and reaction conditions have resulted to a variety of carbon nano-materials (Golnabi, 2012; Mubarak et al., 2014; Rinaldi et al., 2009; Shaikjee & Coville, 2012). CNTs have a wide range of applications due to their novel properties, and further treatments of CNTs make them unique. A 3 trillion US dollar investment is estimated in nanotechnology by 2020 (Roco, Mirkin, & Hersam, 2011). CNT applications cover the area of purification of water, mechanical properties enhancer, pharmaceutical, cleaning materials, electronics, and sensors (Al-Hakami, Khalil, Laoui, & Atieh, 2013; Al-Khaldi, Abu-Sharkh, Abulkibash, & Atieh, 2013; Amr et al., 2011; M. a. Atieh, 2011; M. A. Atieh et al., 2010; Endo, Hayashi, Kim, Terrones, & Dresselhaus, 2004; Girei et al., 2012; Ihsanullah et al., 2015; Mezghani, Farooqui, Furquan, & Atieh, 2011; Tawabini, Al-Khaldi, Atieh, & Khaled, 2010; Zeino, Abulkibash, Khaled, & Atieh, 2014).

Magnetic, dispersive and optical properties of CNT can be enhanced by decorating its surface with metal, metal oxides, organic compounds, and polymer composites. The consequential impregnated CNTs are useful for membrane formation, heavy metals and organic solvents removal from water due to its high surface area and affinity with unwanted materials. Conventional techniques are usually used to synthesize CNT composites with metal/metal oxide (Motshekga, Pillai, Sinha Ray, Jalama, & Krause, 2012).

Impregnation of nano-metals/oxides over CNTs is divided into two eras; the former involves conventional methods of impregnation and the later involves special techniques such as microwave assisted impregnation (Motshekga et al., 2012). Conventional metal/oxide impregnation methods (electro-less deposition, physical evaporation, capillary action, physorption, solid state reaction, colloidal chemistry, radiolysis etc.) involve various steps starting from strong acid treatment to ultras-sonication. Frequently the reduction of metal salts takes hours to days and still particle size and shape of metal/oxide cannot be controlled efficiently (Han & Zettl, 2003; Hull, Li, Xing, & Chusuei, 2006; Mao et al., 2004; Reddy et al., 2006; Xue, Chen, Hong, Lin, & Tan, 2001).

On the other hand microwave assisted impregnation methods are widely used now a days for chemical reactions and nano-material production but this technique is difficult to apply on various metal/oxides (Chen, Lee, & Liu, 2004; Han & Zettl, 2003; Nuchter, Ondruschka, Bonrath, & Gum, 2004; Xu et al., 2007). Because to decompose metal salt into its components, a specific wave-length microwave is required, otherwise it will produce different other compounds of metal/oxide which may be not desired.

To avoid conventional time consuming and difficult techniques we devised a novel *in situ* impregnation process. As our system is based on liquid feed; thus, for in-situ impregnation, metal-salt should be soluble into the solvent of feed solution. Further, this study provides a single step impregnation method which can be easily commercialize by combining scientific research and industrial improvements. A downward co-current feed system is used in a vertical CVD reactor.

p-Xylene (B.P. 138.5 ^{o}C) provides carbon atoms and ferrocene (B.P. 249 ^{o}C) provides iron catalyst. Impregnation of alumina over CNT is discussed in this article to provide an example of this new method. Aluminum isopropoxide is a salt which dissolves in p-xylene. Mekasuwandumrong et al., (Mekasuwandumrong, Kominami, Prasertham, & Inoue, 2004) showed that aluminum isopropoxide decomposes in the presence of hydrocarbons at 600 ^{o}C as follows.

$$Al(OCH(CH_3)_2)_3 \longrightarrow 0.5\,Al_2O_3 + 3\,C_3H_6 + 1.5\,H_2O \quad \text{------- (Eq. 1)}$$

However, Dureas et al., (2007) showed in their work that non-stoichiometric alumina phase ($Al_{2.667}O_4$) can also be produced, due to incomplete crystallization of alumina or due to unexpected temperature variation during the crystallization process (Durães et al., 2007).

Temperature range in our IVCVD reactor varies between 750-900 ^{o}C hence; this high temperature can result in cracking of AIPO to produce Al_2O_3. The in-situ synthesized alumina particles get attach to carbon nanotubes during its synthesis which expected to result in impregnate multiwall carbon nanotubes.

Studies have shown that the deposition of metal nanoparticles onto the surface of CNTs can not only protect these particles from aggregation, but also improve their catalytic activities, and even produce properties that are not accessible to CNTs and metal nanoparticles alone, which are important for their use in water purification techniques. (S. W. Lee, Kim, Chen, Shao-Horn, & Hammond, 2009; S. Wang, Jiang, White, Guo, & Wang, 2009; Wu et al., 2009; Zhao, Fan, Zhong, Li, & Yang, 2007)

The basic purpose of impregnation of MWCNT is to enhance its surface area and to disperse alumina over its surface to produce active sites. These active sites help in capturing of heavy metals in bundles of MWCNTs. Therefore, reaction was run at different combination of H_2 and Ar, temperature and reaction time. Effect of these parameters is investigated by characterizing produced impregnated CNTs using scanning electron microscopy (SEM), transmission electron microscopy (TEM), thermo gravimetric analysis

CHAPTER 3

FABRICATION, MATERIALS AND METHODS

A vertical CVD reactor was used for the production of CNT. The reactor was made of quartz tube with a collector at the bottom. In this chapter, fabrication and design of the reactor are briefly explained whereas experimental detail and characterization methods are discussed in detail.

3.1 FABRICATION OF (CR-CVD)

Our aim was to fabricate a very advanced and sophisticated Semi-Continues Reaction Chemical Vapor Deposition (CR-CVD) reactor with simple features at a reasonable cost, in order to produce pure and high yield of CNT. The design methodology is schematically described in Figure 3.1.

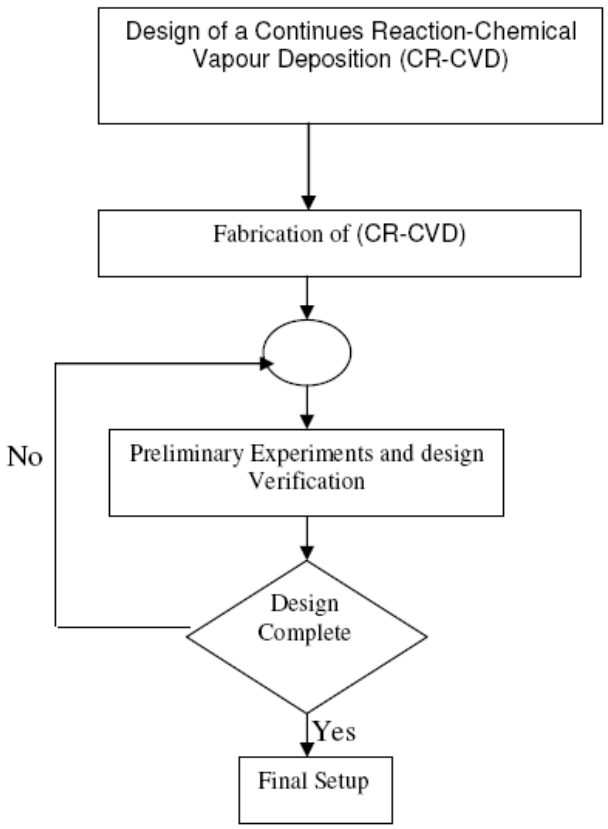

Figure 3.1: Methodology for the development of a new instrument (CR-CVD)

3.1.1 Design of Injection Vertical Chemical Vapor Deposition (IV-CVD) Reactor

This section elaborates the mechanism to design and fabricate the IV-CVD reactor. Ultimate use of this reactor is to produce carbon nanotubes using fluidization method. Figure 3.2 indicated the framework picture of the IV-CVD reactor. Reactor is made from quartz tube which is placed vertically. Flanges are used to pack the quartz tube of the reactor from both ends to avoid any leakage of gases.

Feed is injected from top of the reactor in the form of liquid drops or atomized spray. Carrier gas takes the atomized-feed to the reaction zone. Temperature of the reaction zone is controlled by electric furnace which heats the reactor gradually. The synthesize CNT deposits on the quartz wall of the reactor. A collector box is designed at the bottom end of the reactor. After completion of reaction, synthesized CNT is scrapped from the quartz wall and then collected from the collector. Effluent gases leave from bottom of the reactor. Reaction parameters such as; reaction temperature, gases flow rate and injection rate of feed can tuned to optimize yield.

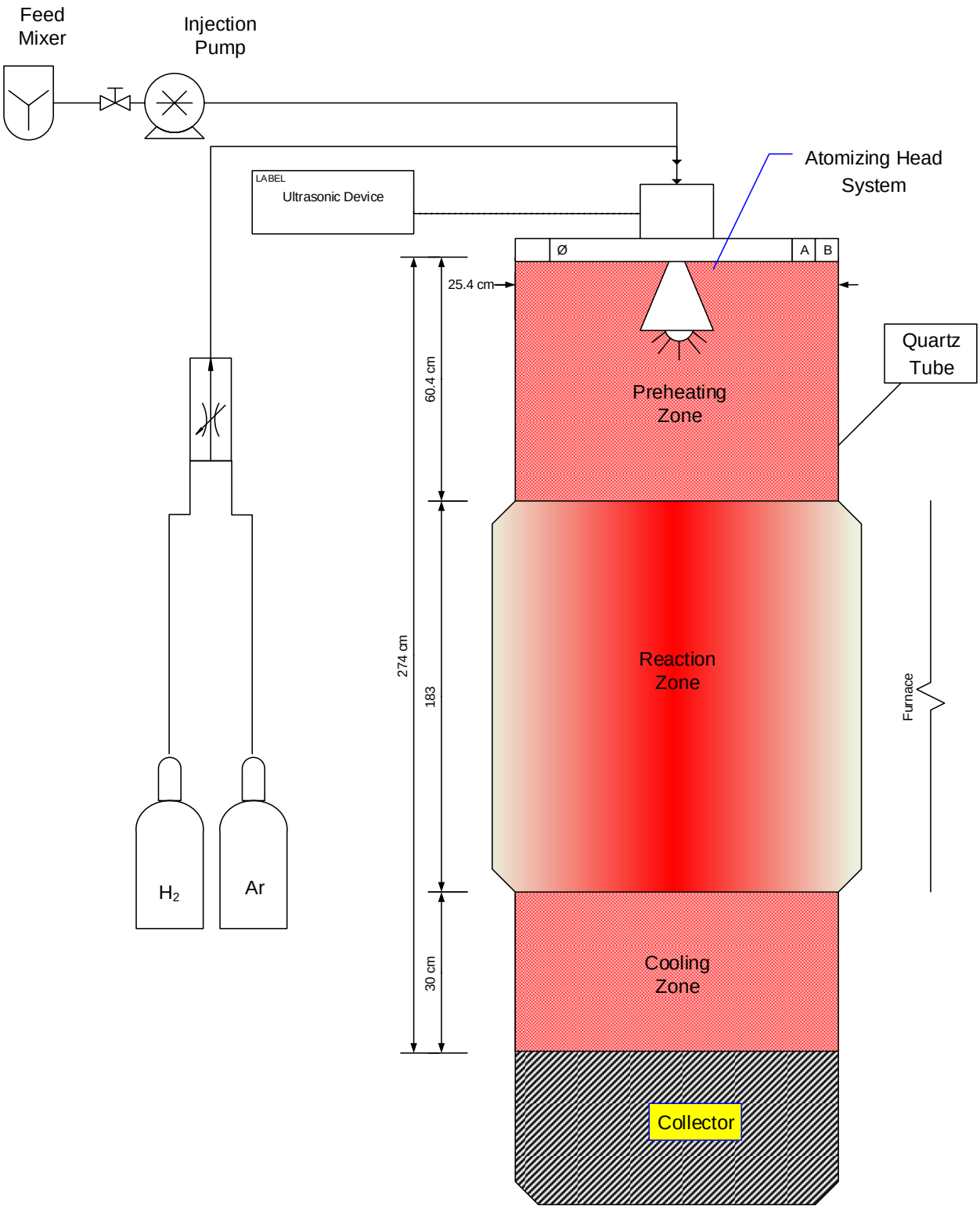

Figure 3.2: Schematic Diagram of the Designed IV-CVD Reactor

3.2 Materials

p-Xylene (pX, C_8H_{10}, 96-99%) was purchased from Sigma-Aldrich Co. LLC. and was used without further purification. Ferrocene (FCN, $(C_5H_5)_2Fe$) was purchased from Honeywell Riedel-de Haen International Inc. with 96-99% purity and was used without further purification. Aluminum isopropoxide (AIPO, $C_9H_{21}AlO_3$, 98-99 %) was purchased from Acros Organics, USA and was used such as. Hydrogen (H_2, 99.9990%) and argon (Ar, 99.996%) were purchased from local supplier.

3.2.1 Reaction & Carrier Gases

Hydrogen and argon gases were used as a reaction gas and a carrier gas respectively. Digital mass flow controllers were used to control the flow rate of both gases.

3.2.2 Impregnation of Alumina over MWCNT Surface

AIPO is a salt of aluminum which produces Alumina on pyrolysis at high temperature in the presence of higher hydrocarbons. Therefore, AIPO is dissolved in p-xylene and injected into the reactor for in-situ impregnation of alumina over surface of MWCNT.

3.2.3 Precursor & Catalyst

pX acted as a precursor and provided carbon atoms which were building blocks for CNT. FCN provided Fe, which was a catalyst for CNT formation. The feed solution (FS) containing pX and FCN was injected at a constant flow rate into the IVCVD reactor by using syringe pump. AIPO was used to produce Al_2O_3 which impregnated on CNT during synthesis process.

3.2.4 Atomization

Feed will be converted into droplets by a special type of atomizer which sprays the catalytic solution along with the reaction gases, through internal-mix two-fluid nozzles into the vertical reactor. Ultrasonic atomization system, consisting of wide range atomizing nozzle and frequency generator of 20 kHz, was bought from Sonaer Inc. The atomizer has advantage over other types as it is operated by ultrasonic meter which controls the droplet size, size distribution, trajectory and speed that in turn determine that final character of the particle. Figure 3.3 indicates the velocity profile of feed solution which is formed by the ultrasonic atomization.

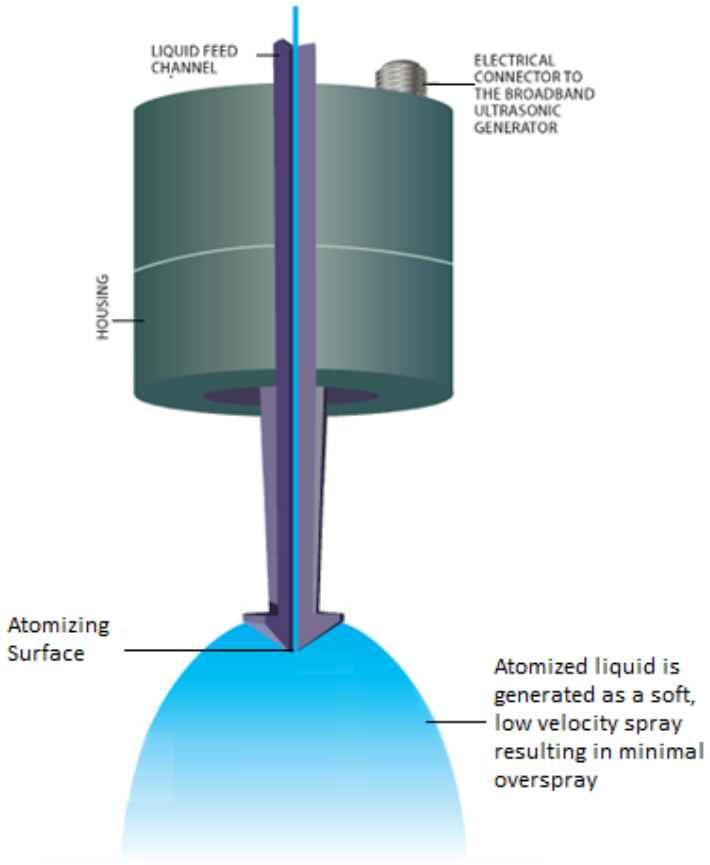

Figure 3.3: Velocity profile of feed solution from the atomizer nozzle. [http://www.sono-tek.com]

3.3 Methods

3.3.1 MW-CNT Synthesis by Using p-Xylene and Ferrocene

The experimental set-up used to synthesize MWCNTs is shown in Figure 3.2. Argon was purged into the reactor to remove any unwanted gas. The reactor was heated under argon atmosphere to 850 ^{o}C by an electric furnace with a temperature increment of 10 ^{o}C/min. One weight percent solution of FCN into pX was prepared, taken into a syringe and then placed in an injection pump. An ultrasonic atomization system was installed at the top head of reactor, which operated at high frequency, 20 kHz, to obtain smallest droplet size. FS passed through atomization nozzle and spread in the reactor in an *umbrella-shape* profile. This injection system makes evenly distribution of FS particles. This type of feed injection system is a new technology that was used for the first time for CNT production, up to our knowledge. Previously this system was used for cracking of higher hydrocarbons to lower hydrocarbons.

Argon, the carrier gas (CG), took the atomized FS to the reaction zone of the reactor. H_2 was introduced into the reactor from top when deposition of FS on the quartz wall of reactor was observed. Flow rate ratio of H_2: Ar was kept at 3:1. Reaction proceeded and depositions of CNTs on the quartz wall of reactor were observed. Effluent gases left from bottom of the reactor into atmosphere. After completion of reaction, system was cooled down to room temperature in Ar atmosphere. Reaction was run at different temperatures ($T_{R,}$ 750 to 950 ^{o}C), injection flow rate of FS (60, 75, and 90 mL/h) and without carrier gas (only flow of H_2 was varied).

3.3.2 IM-CNT Synthesis by Using p-Xylene, Aluminum Isopropoxide and Ferrocene

The same procedure was followed to prepare IM-CNT except:

1. Aluminum Isopropoxide (AIPO) was also used.
2. The feed solution consisted of w/w; 98 % p-Xylene, 1 % AIPO and 1% FCN

The reaction was run at different condition as described before.

3.3.3 Calculation of Yield

Alimorad R. et. al. (2011) proposed a formula which was used for yield calculation (Rashidi, Lotfi, Fakhrmosavi, & Zare, 2011).

$$\text{Yield } (\eta) = \frac{W_{(cat+CNT)}}{W_{pre}} \; x \; 100$$

Where

$W_{(cat + CNT)}$: weight of synthesized CNT (g)

$W_{(pre)}$: weight of precursor (g)

3.3.4 Analytical Investigations

The synthesized CNT was collected from the reactor wall in the form of powder or flakes and then was weighed for yield calculation. Scanning electron microscope (SEM, TESCAN MIRA 3 FEG-SEM) was used to determine the morphology of CNT whereas

to characterize the CNT, transmission electron microscope (TEM, Field emission electron microscope JEM-2100F) was used.

3.3.5 Purity Measurement

Thermal gravimetric analyzer (K.U. Leuven SDT, Q600) was used to conduct TGA purity measurement of CNT. Sample was oxidized in oxygen environment from room temperature to 850 ^{o}C at the heating rate of 10 ^{o}C per minute. TGA analysis was made on the basis of weight loss as a result of temperature increment. The residue obtained after complete oxidation determined the purity and thermal stability of sample.

3.3.6 BET Analysis

Brunauer-Emmett-Teller (BET) theory targets the phenomenon of physical adsorption and desorption of gas molecules on a solid surface. BET analysis was made by micropore analyzer (Quantachrome, Autosorb IQM0000-4) which calculates the exact specific surface area of materials by comparing adsorption of nitrogen against relative pressure by using complete automated analyzer. The technique incorporates pore area and external area to find out the total specific surface area in m^2/g.

3.3.7 XRD

X-ray diffraction is used to determine the atomic and molecular forms of elements present in a material. When X-rays beam passes through a material then the crystalline atoms deflect it into many particular directions. Density of electrons inside a crystal is calculated by measuring the angles and intensities, which in-turns provides the

information about chemical bonds, molecular structure, disorder, crystallinity, phase identification and various other information.

In this work MW-CNT and IM-CNT were characterized by using Desktop X-ray Diffractometer (XRD, Miniflex II). A prescribed amount of sample of material was taken on glass-slit and after spreading uniformly, it was inserted into the machine where 2-theta rate was fixed. After complete scanning of sample, the data was analyzed by determining different peaks overlapping methods.

3.3.8 Thermal Properties

To determine thermal properties of MWCNT, different percentage solutions of MWCNT into water (0.1, 0.3 and 0.5 weight percent) were prepared and mixed thoroughly using ultrasonic sonication. Arabic Gum (AG) was also added along with MWCNT into solution prior to sonication with the ratio of 2:1 respectively. MWCNT was hydrophobic by nature, so to disperse it into water AG was used.

CHAPTER 4

SYNTHESIS OF HIGH PURITY, HIGH ASPECT RATIO MULTIWALL CARBON NANOTUBES BY USING VERTICAL CVD REACTOR

4.1 Results & Discussions

Three reaction parameters i.e., crucial role of H_2, optimization of reaction temperature, and effect of reaction time, were studied. Initial analysis of CNT was made on the basis of yield obtained after each experiment. On the basis of high yield; SEM and TGA was run. SEM analysis was performed using field emission scanning electron microscope (TESCAN MIRA 3 FEG-SEM) which provided the structure and alignments of CNTs. Length of CNT bundles and aspect ratios at different reaction conditions were also made on the basis of SEM analysis. Thermogravimetric analyzer (K.U. Leuven SDT, Q600) was used to perform TGA at a heating rate of 10 ^{o}C/min in air. Purity of CNT is described as the non-ash content present in the sample of CNT. Non-ash content in the samples is iron (catalyst) which can be removed by acid treatment. But in this article we characterized as synthesized MWCNT to study unmodified properties of product. TEM analysis was performed using field emission electron microscope (JEM-2100F) which

provided information about single MWCNT pattern, number of walls, and space between walls, catalyst shape and place inside MWCNT. Surface area of MWCNT was measured by a surface area analyzer (Micrimeritics, Norcross GA) in Nitrogen atmosphere with a 15-point BET at 77 K.

4.2 Crucial Role of Reaction Gas (H_2)

Figure 4.1 shows the data obtained by varying H_2 and Ar flow rates in a way that the total flow rates of both gases will be 4.0 L/min. Thus by increasing hydrogen flow rate will result in decrease of argon flow rate. Temperature and reaction time of the system were kept constant at 850 ^{o}C and 30 min respectively. CNT yield increases by increasing H_2 flow rate until it reaches a maximum value of 7.4 % at 3 L/min. A further increase in H_2 flow rate does not materially affect the yield. Increase in yield from lower flow rates to higher flow rates is due to the reducing nature of H_2.

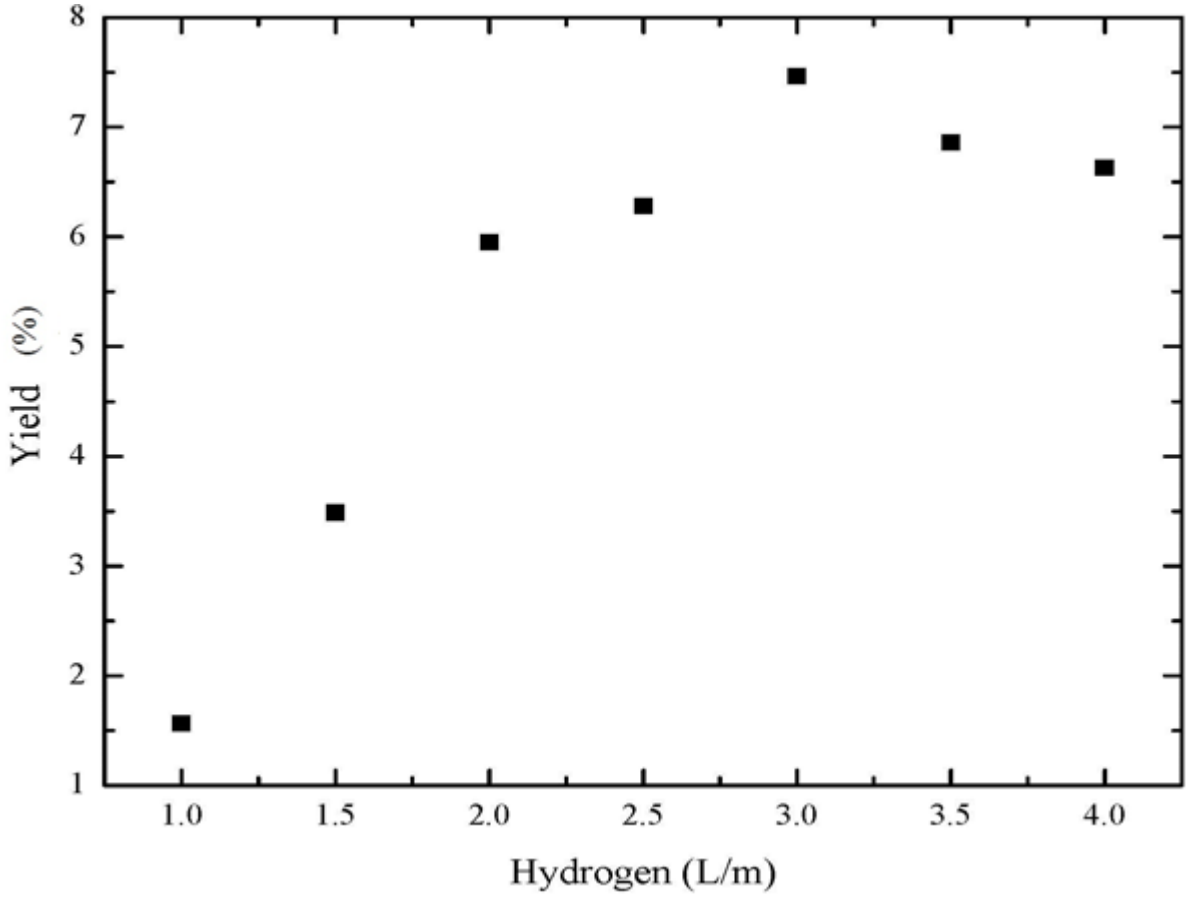

Figure 4.1: Yield of CNT obtained by varying flow rate of H_2, and keeping constant temperature and reaction time at 850 ^oC and 30 min respectively

p-Xylene (C_8H_{10}) and ferrocene ($C_{10}H_{10}Fe$) crack to form atomic carbon and iron in the presence of a reducing agent. Hence the concentration of H_2 in the reactor accelerates the CNT formation (Rashidi et al., 2011; Singh, Shaffer, & Windle, 2002). But if the concentration of H_2 will reach to its saturation point then further increase in H_2 will start decelerate the CNT formation (Figure 4.1). In our system the saturation of H_2 reached at 3.0 L/min and maximum yield was obtained at this point. Then further increase in hydrogen flow rate did not enhance the yield but rather it started decreasing. It is because at higher concentration, hydrogen started reacting with carbon to produce lower hydrocarbons which caused low yield. It was observed from SEM images that although yield decreased at 4.0 L/min flow rate of H_2 as compared to 3.0 L/min, but very aligned and large bundles of carbon nanotubes were obtained that were not present at other conditions (Figure 4.2).

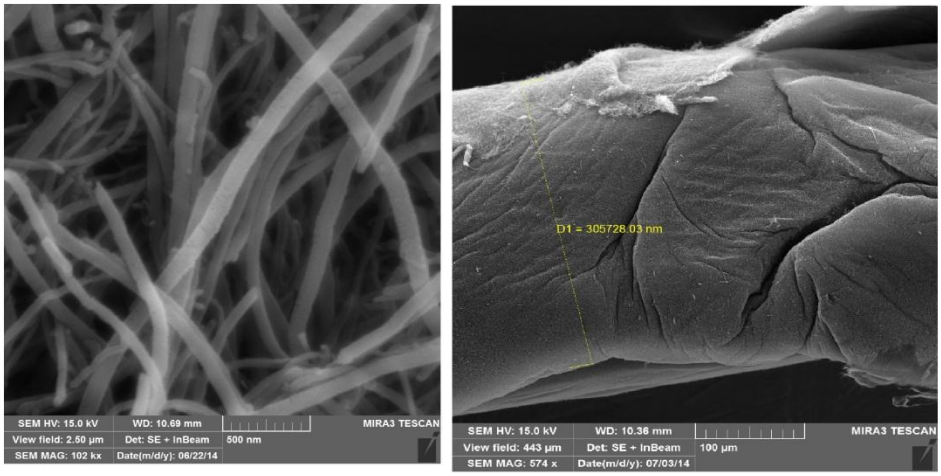

Figure 4.2. SEM image of MWCNT obtained at 850 ^oC temperature, 3.5 L/min H_2 flow rate, 30 min feed reaction time and without any carrier gas.

The synthesized CNT samples that were obtained at higher H_2 flow rates (3, 3.5 and 4 L/min), were analyzed through thermo gravimeteric analysis (TGA). A 5 mg sample was

oxidized in an oxygen environment at a heating rate of 10 ^{o}C/min. Results are shown in Figure 4.3. The figure indicates that a sharp decrease in percent weight loss of CNT occurred between temperature range 500-600 ^{o}C. Bom et al. (2002) described that maximum weight loss of MWCNT in the above range of temperature is evidence of presence of single and multiwall carbon nanotubes (Bom et al., 2002). Further increase in temperature removed all carbon from samples and about 4 % residue remained after complete analysis. High purity of CNT is due to the ideal of ferrocene to p-xylene ratio and perfect dispersion of the feed solution into the IVCVD reactor by using the ultrasonic atomized technology.

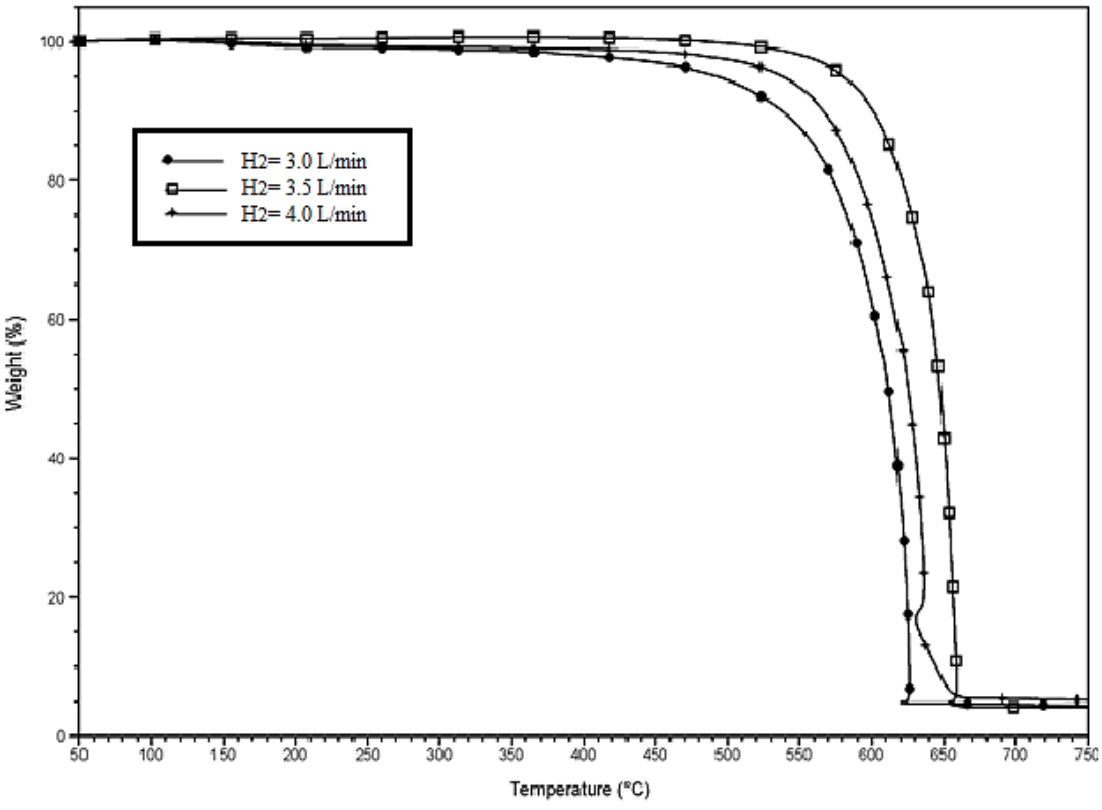

Figure 4.3: TGA of CNT obtained by changing hydrogen flow rates

4.3 Optimization of Reaction Temperature

Reaction temperature plays a very important role in CNT morphology and yield, as it controls the size of the catalyst, which in turn controls the diameter and aspect ratio of CNTs. Ferrocene (the catalyst) is an organometallic compound which produces Fe particles by thermal cracking at 600 ^{o}C (Koprinarov, Konstantinova, Ruskov, & Spirov, 2007). After decomposition, Fe particles agglomerate due to intra-molecular forces. In this work temperature was varied from 750 to 950 ^{o}C, which is higher than the decomposition temperature of ferrocene. Kinetic studies at atomic level illustrate the idea of diffusion by collision. This means that at high temperatures molecules will collide frequently to form larger particles than those formed at lower temperatures. Hence, the diameter of MWCNT should increase at higher temperatures as described by different authors (Koprinarov et al., 2007; Singh et al., 2002; Tapasztó et al., 2005).

The reaction temperature was varied from 750 to 950 ^{o}C while keeping all other conditions constant: feed flow rate 90 mL/h, H_2 flow rate 3 L/min and Ar flow rate 1 L/min. Yield analysis from Figure 4.4 indicates that: the yield increased from 1% at 750 ^{o}C to 7% at 850 ^{o}C. A further increase in temperature to 950 ^{o}C decreased the yield to 5.8%.

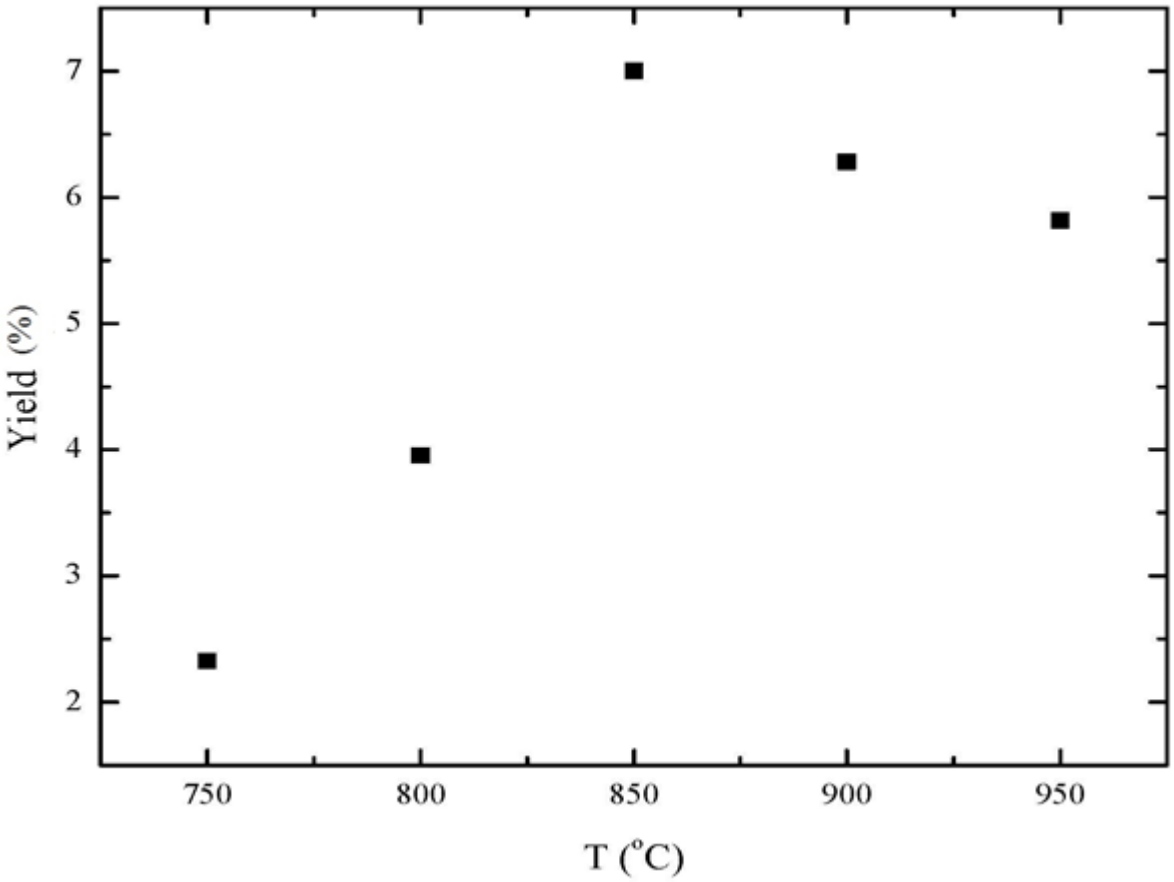

Figure 4.4: Yield of CNT obtained by varying reaction temperature, and keeping constant H_2 flow rate and reaction time at 3 L/min and 30 min respectively

SEM analysis of MWCNT indicates that at 750 ^{o}C, CNT contains some unreacted particle (Figure 4.5. a, b). These unreacted particles were not present when temperature was raised to 800 ^{o}C and even an aligned structure of CNT appeared (Figure 4.5. c, d). Length of CNT bundles increased further when reaction was run at 850 ^{o}C (Figure 6. e, f). Increasing the temperature further above 900 ^{o}C resulted in the destruction of the CNT bundles and again impurity starting appearing at 750 ^{o}C (Figure 4.5. g, h, i and j).

TEM analysis was run for the sample which was obtained at 850 ^{o}C (Figure 4.6 a). Catalyst particle on the tip of the MWCNT indicates that CNTs were formed due to a tip growth mechanism. Multilayers of walls are visible as well (Figure 4.6 b, c).

.

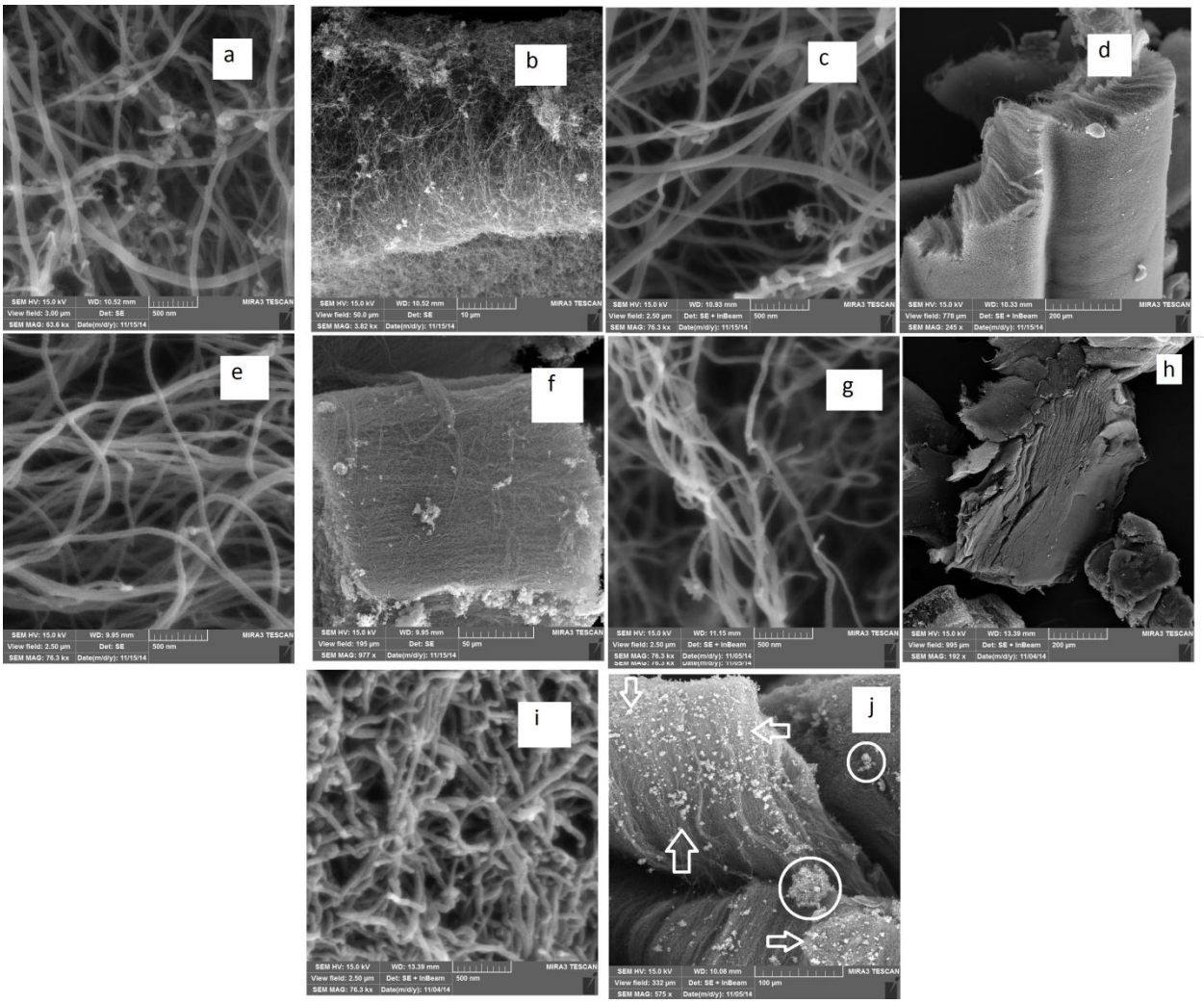

Figure 4.5. High and low resolution SEM images of MWCNT obtained at different temperatures. (a,b) at 750 ^{o}C, (c,d) 800 ^{o}C, (e,f) 850 ^{o}C, (g,h) 900 ^{o}C, (I,j) 950 ^{o}C and 3 L/min H_2 flow rate, 1 L/min Ar flow rate, and reaction time 30 min.

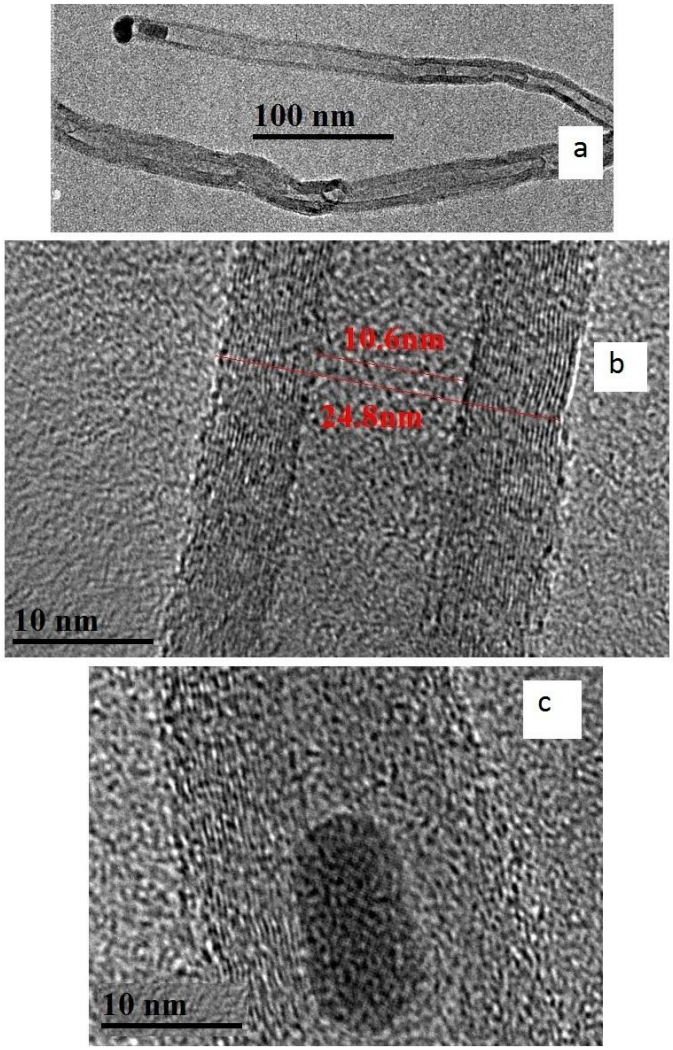

Figure 4.6 HRTEM image of one MWCNT a) complete tube, b) multi-tubes of carbon are visible, inner and outer diameters are measured, c) shape of catalyst particle inside MWCNTs

The diameters of MWCNTs, which were synthesized at different temperatures (i.e., 750, 800, 850, 900, and 950 ^{o}C), were measured by SEM at three different locations. The data obtained are shown in Figure 4.7.

There is a large difference in the diameter range of MWCTs at 750, 800 and 850 ^{o}C. But this difference narrows at 900 and 950 ^{o}C. Jin et al. (2001) (Jin et al., 2001), and Lee et al. (2002) (C. J. Lee et al., 2002) found the diameter of Fe particles at 850 ^{o}C and 950 ^{o}C as 90 ± 20 nm and 150 ± 40 nm respectively. Corresponding diameters to above temperatures were 60 ± 10 and 130 ± 20 nm. However, our results showed smaller diameters; 45 ± 10 and 50 ± 10 nm at 900 ^{o}C and 950 ^{o}C respectively. These small diameters could be a result of a larger dispersion area in the reactor and a shorter residence time at higher temperatures.

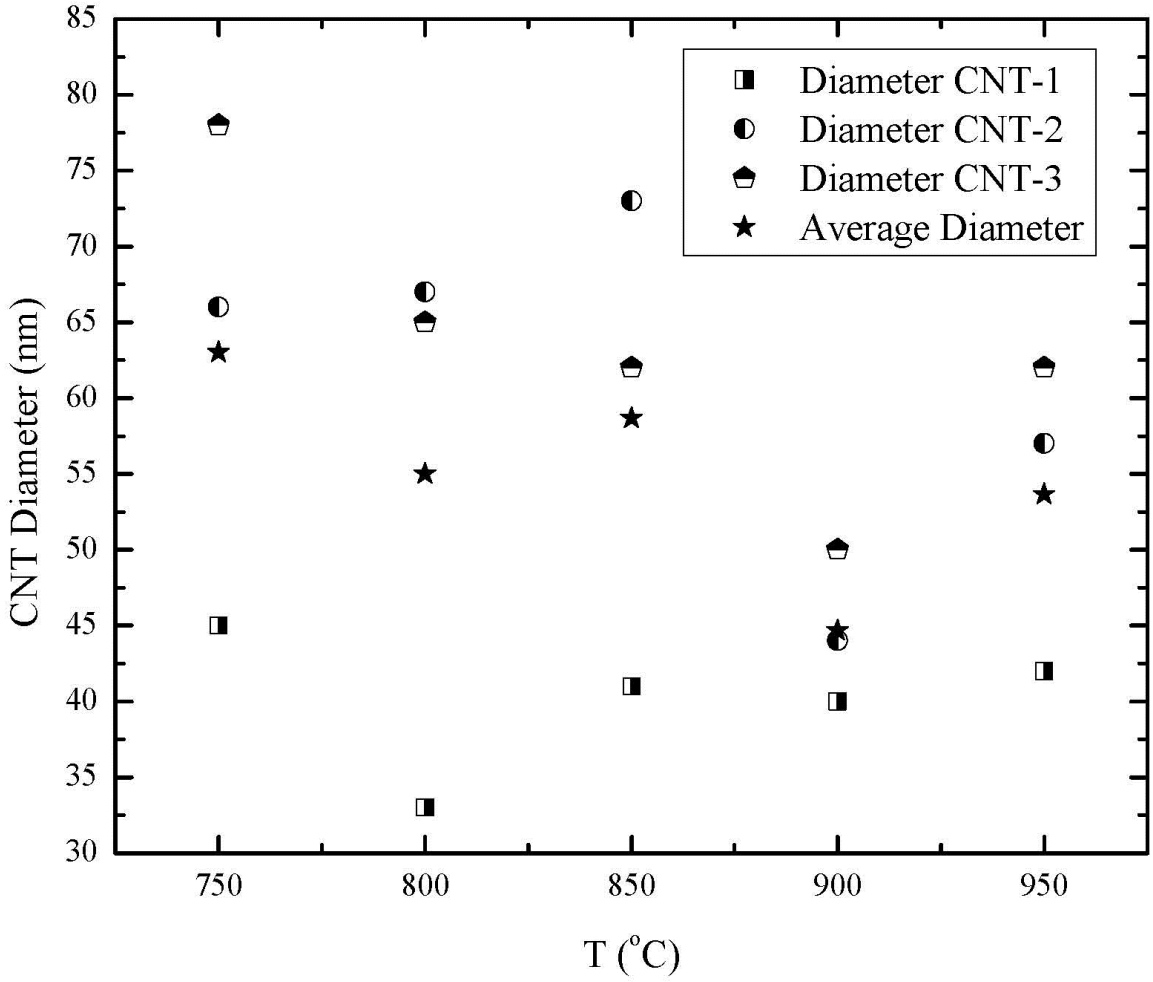

Figure 4.7: Diameter distribution obtained by different runs at different temperatures

TGA of yield obtained at different temperatures is shown in Figure 4.8. Samples of CNT collected at 750-900 ^{o}C show similar behavior of oxidation and 94 ± 2 percent pure yield was obtained depending on purity present in the samples. But strange behavior of weight loss was observed for the sample obtained at 950 ^{o}C. Detail sample analysis indicated that this weight loss was due to the presence of inactive agglomerated catalyst particles of iron which behaved as an impurity in the sample. Therefor metallic particles of iron absorbed heat when it was exposed to heat inside the furnace and resulted in fast oxidation of MWCNT. These agglomerated particles were also observed in SEM analysis (Figure 4.5 i and j).

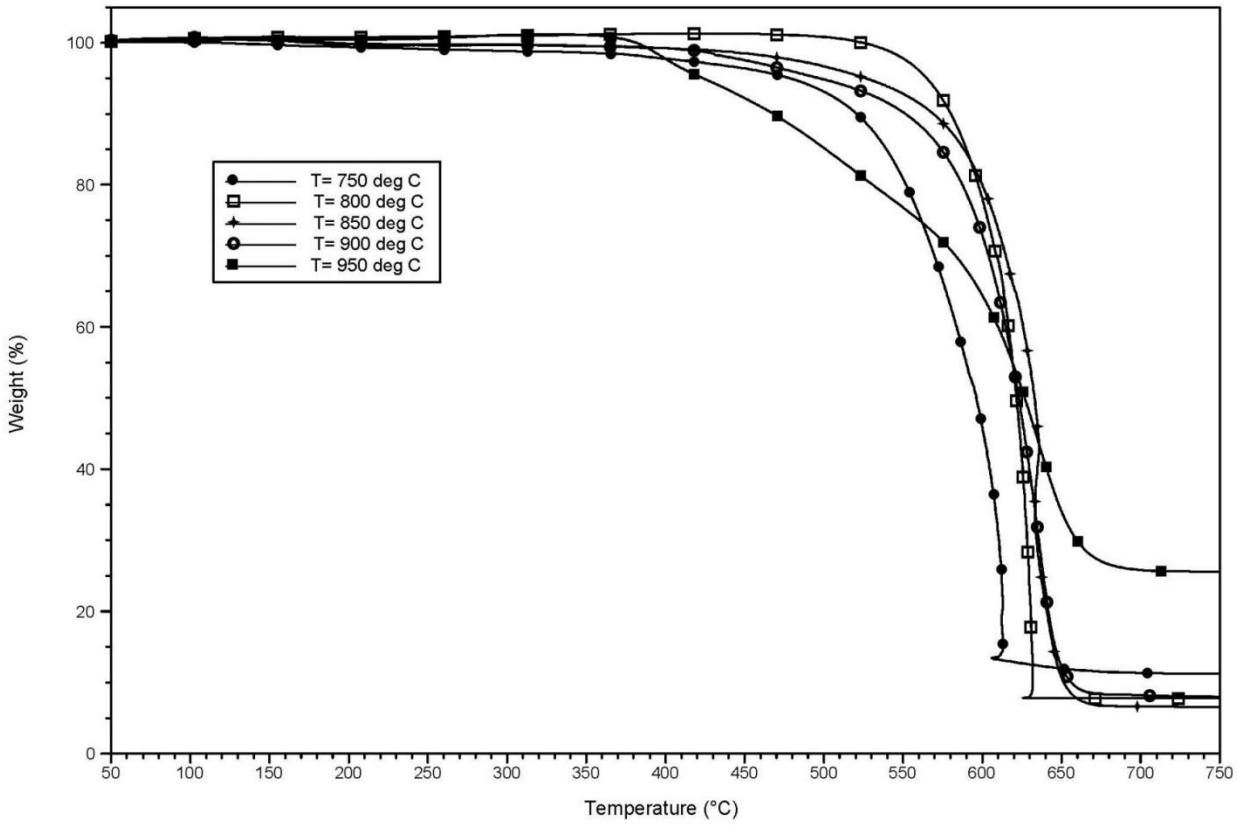

Figure 4.8: TGA of CNT obtained by changing reaction temperature

4.4 Reaction Time Effect

Reaction time of MWCNT was varied by changing the injection rate of 50 mL feed solution. Length of MWCNT can be controlled by selecting an appropriate reaction time. So to study its effect, the reaction was run for 30, 45 and 60 minutes. Figure 4.9 represents the data of yield obtained. Although yield increased by increasing reaction time but it is obvious from the figure that the quantity of MWCNT in each run did not differ a lot from each other. An average of 6.77 ± 0.4 % of yield was obtained. These results indicate that reaction time has not a sufficient effect on yield obtained in our vertical CVD reactor. This is contrast to other results using CVD reactors, in which fluidized beds or floating catalyst techniques have been used and yield is affected by varying run duration (Venegoni et al., 2002).

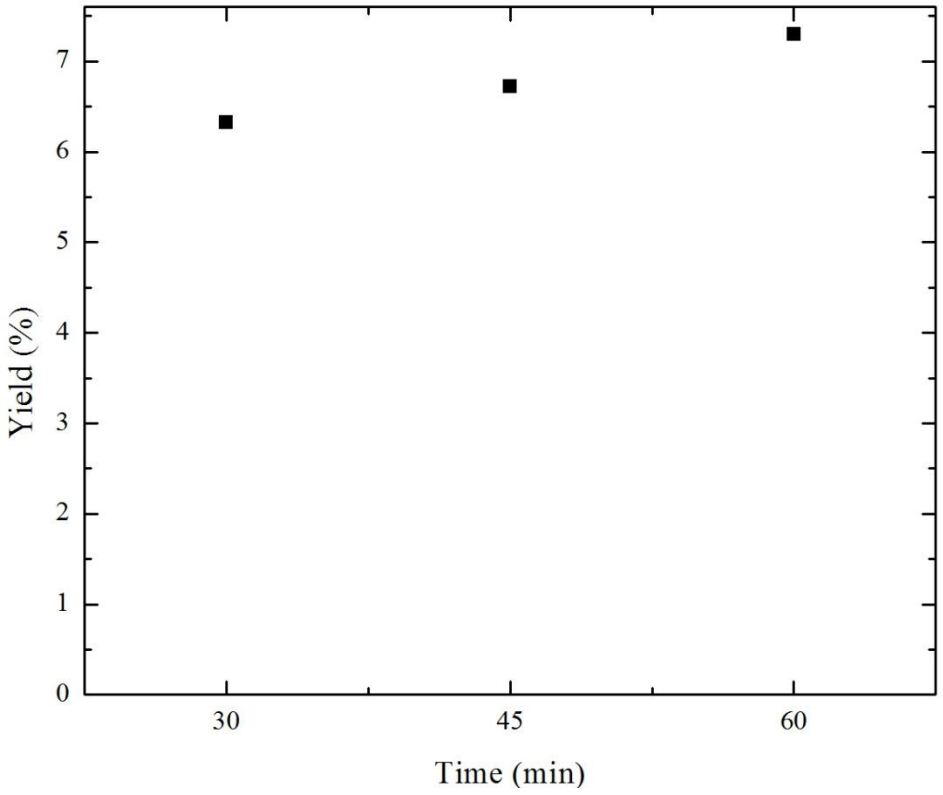

Figure 4.9: Yield of CNT obtained by varying reaction time, and keeping constant temperature and flow rate of H_2 at 850 ^oC and 4 L/min respectively

Results obtained by TGA analysis of the CNT are shown in Figure 4.10. Complete oxidation of CNT resulted in weight loss of carbon content of CNTs, unless all carbon oxidized to CO_2. On the basis of weight loss of carbon content we found that more than 96 % pure CNT was produced. Remaining ash content was the catalyst used to synthesize CNT.

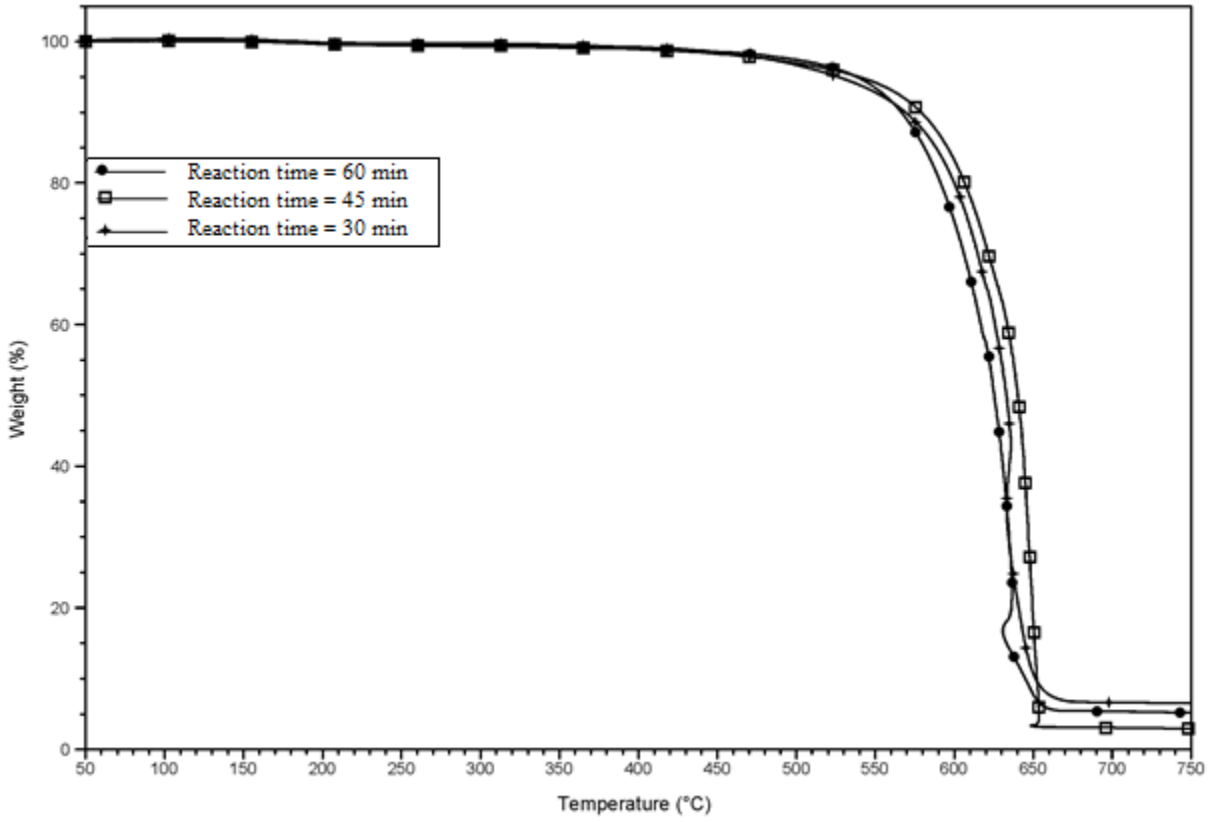

Figure 4.10: TGA of CNT obtained by changing feed reaction time

CHAPTER 5

SYNTHESIS OF VERY HIGH SURFACE AREA Al_2O_3 IMPREGNATED MULTIWALL CARBON NANOTUBES

5.1 Results And Discussions

Impregnated multiwall carbon nanotubes (IM-CNT) were synthesized by the method described in Chapter 3, Section 3.3.3. Hydrogen gas was used as a reaction gas to provide reducing environment for the pyrolysis of p-xylene and ferrocene in the presence of aluminum isopropoxide. Different ratios of hydrogen and argon were used to study in-detail behavior of synthesized impregnated multiwall carbon nanotubes. Role of reaction temperature was also studied and a comparison is made to synthesize uniform diameter impregnated MWCNT. Finally feed was injected into reactor at different flow rates to increase/decrease reaction time. The synthesized IM-CNT was characterized by using SEM, TEM, EDS, TGA, BET and XRD.

5.2 Yield Percent to Optimize Reaction Parameters

Reaction was run at different conditions to reach to the optimum conditions where high yield could be obtain. The data obtained is shown in Table 1. Run 1 to run 7 indicates the results in which flow rates of hydrogen and argon were varied by keeping constant reaction temperature and time to 850 ^{o}C and 30 minutes respectively. A large variation of yield was observed when hydrogen flow rate was increased from 1 to 3 L/min until maximum yield of 4.93 percent could be obtained at hydrogen and argon flow rates of 3:1 respectively. A further increase in hydrogen flow rate decreased the produced CNT quantity.

Temperature of the reactor was varied from 750 ^{o}C to 950 ^{o}C from run 8 to 12. Other parameters were kept constant, hydrogen flow rate, argon flow rate and reaction time to 3 L/min, 1 L/min, and 30 minutes respectively. Reaction time was varied 30, 45 and 60 minutes to further optimize reaction parameters (Run 13-15). It was observed that temperature and reaction time did not affect the synthesis of impregnated MWCNT a lot and an average of 4.46 % yield was obtained. The main parameter which governed the optimum condition was flow rate of hydrogen.

Table 5-1: Yield percent of various experiments at different reaction condition

RUN #	H_2 (L/m)	Ar (L/m)	Temp (^oC)	Time (min)	Yield (%)
1	1	3	850	30	1.627
2	1.5	2.5	850	30	2.051
3	2	2	850	30	3.469
4	2.5	1.5	850	30	4.232
5	3	1	850	30	4.930
6	3.5	0.5	850	30	4.255
7	4	0	850	30	4.186
8	3	1	750	30	3.186
9	3	1	800	30	5.412
10	3	1	850	30	4.930
11	3	1	900	30	4.697
12	3	1	950	30	4.697
13	3	1	850	60	3.755
14	3	1	850	45	4.085
15	3	1	850	30	4.930

5.3 EDS, XRD & TGA analysis

EDS analysis was used to detect metals present in the sample. Results obtained are shown in Figure 6. Carbon is building block of CNT and it was found to be 67.8 % weight of total sample. Iron is catalyst for CNT and it was found to be 8.2 weight percent whereas; aluminum and oxygen were found to be 11.2 and 12.9 weight percent respectively. Simple stoichiometric ratio of aluminum and oxygen was not 3 and 2 to form Al_2O_3. Hence other forms of oxide of aluminum were also present in the sample.

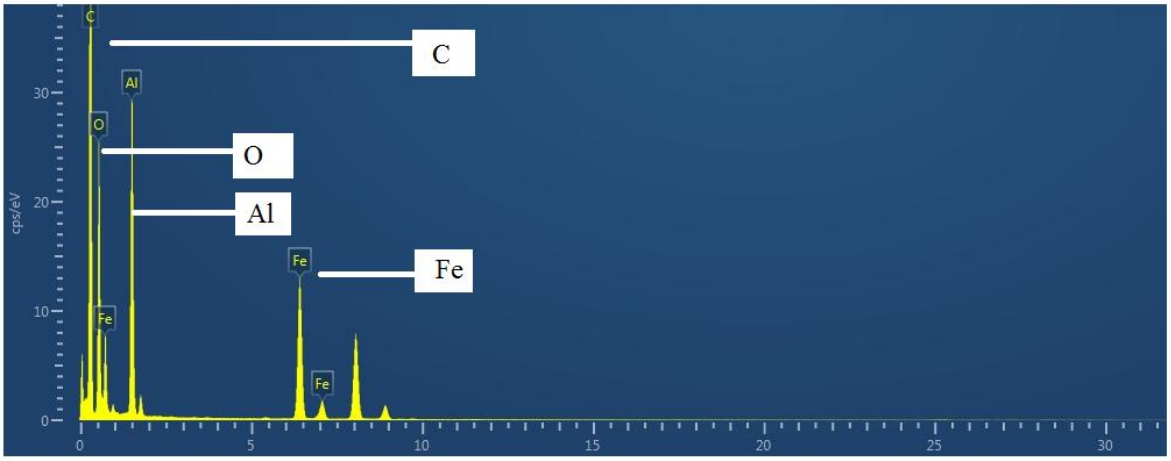

Figure 5.1: EDS analysis of impregnated MWCNT

XRD (Desktop X-ray Diffractometer, Miniflex II, XRD) was used to identify the atomic and molecular structure of aluminum and oxygen present in the sample. The results obtained are shown in Figure 7. Different peaks were obtained based on regularity and symmetry of sample. One main peak at 25.88 shows the presence of carbon in the form of multiwall carbon nanotubes. Other low intensity peaks represent the presence of oxides of aluminum. Phase and molecular form of elements present in the samples were found by built-in peak fitting technique of XRD-instrument. It was observed that

aluminum and oxygen are present with different ratios. Mostly Al_2O_3 in corundum phase was present in the sample, but a non-stoichiometric alumina phase $Al_{2.667}O_4$, was also found. Dureas et al., (2007) showed in their work that non-stoichiometric alumina phase ($Al_{2.667}O_4$) can be the result of incomplete crystallization of alumina or unexpected temperature variation during the crystallization process resulting from Eq. 1 (Durães et al., 2007). This behavior explains the imbalance atomic weight percent obtained by EDS analysis (Figure 6)

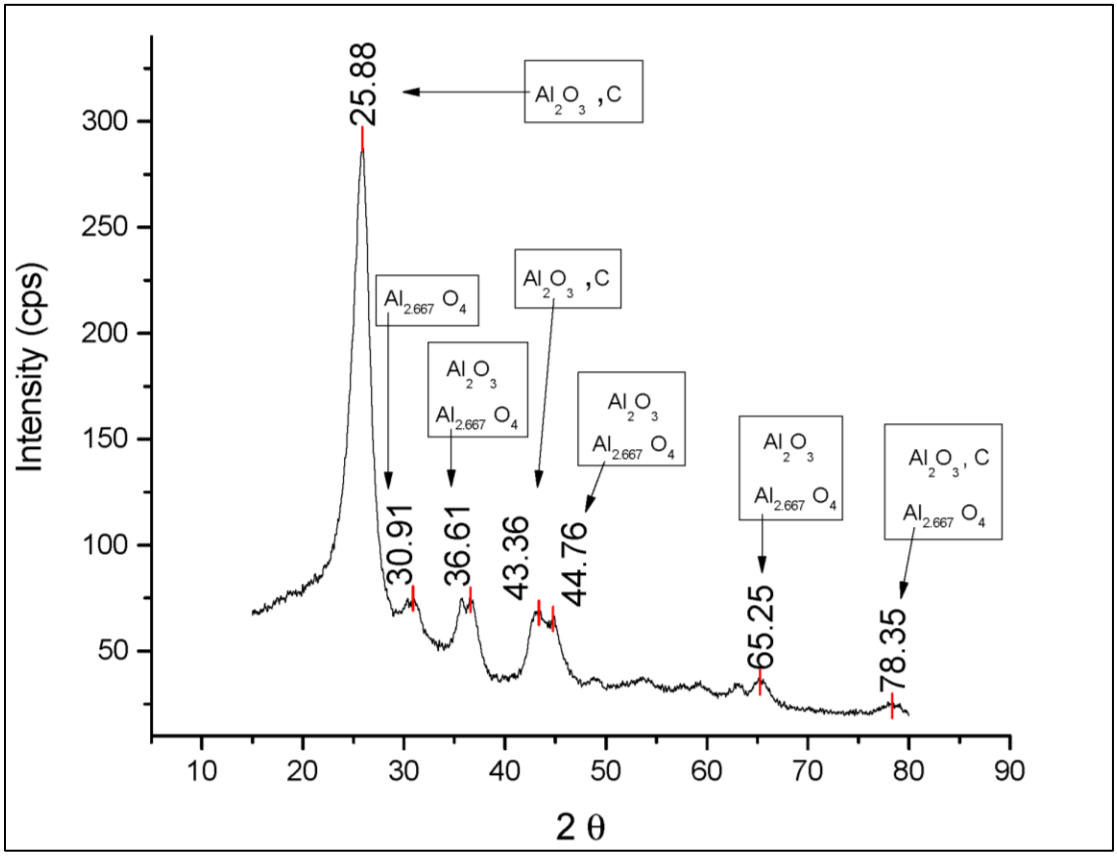

Figure 5.2: XRD analysis of synthesized impregnated MWCNT

Thermal gravimetric analyzer (K.U. Leuven SDT, Q600) was used to conduct TGA purity measurement of CNT. Sample was oxidized in oxygen environment from room temperature to 850 ^{o}C at the heating rate of 10 ^{o}C per minute. TGA analysis was made on the basis of weight loss as a result of temperature increment. The residue obtained after complete oxidation determined the purity and thermal stability of sample.

Figure 3 indicates the TGA analysis of pure and impregnated MWCNT. It can be seen that pure MWCNT is thermally stable as compare to impregnated MWCNT. Oxidation of pure MWCNT starts at 575 ^{o}C whereas that of impregnated MWCNT starts at 450 ^{o}C. The decrease in oxidation temperature of impregnated MWCNT can be due to alumina particles which are present over the surface of MWCNT and act like a heat reservoir to decrease the oxidation temperature. Whereas no such particles are present on case of pure MWCNT therefore a sharp decrease in weight loss can be observed until the whole sample oxidized at 650 ^{o}C leaving 5 % residue. This 5 % residue was merely the catalyst particles which were used to synthesize MWCNT.

The complete oxidation temperature of impregnated MWCNT is also 650 ^{o}C as that of pure MWCNT; but a large amount of residue remained. The residue obtained after complete oxidation indicates the non-oxidized material present in the sample; in this case it is alumina and iron particles.

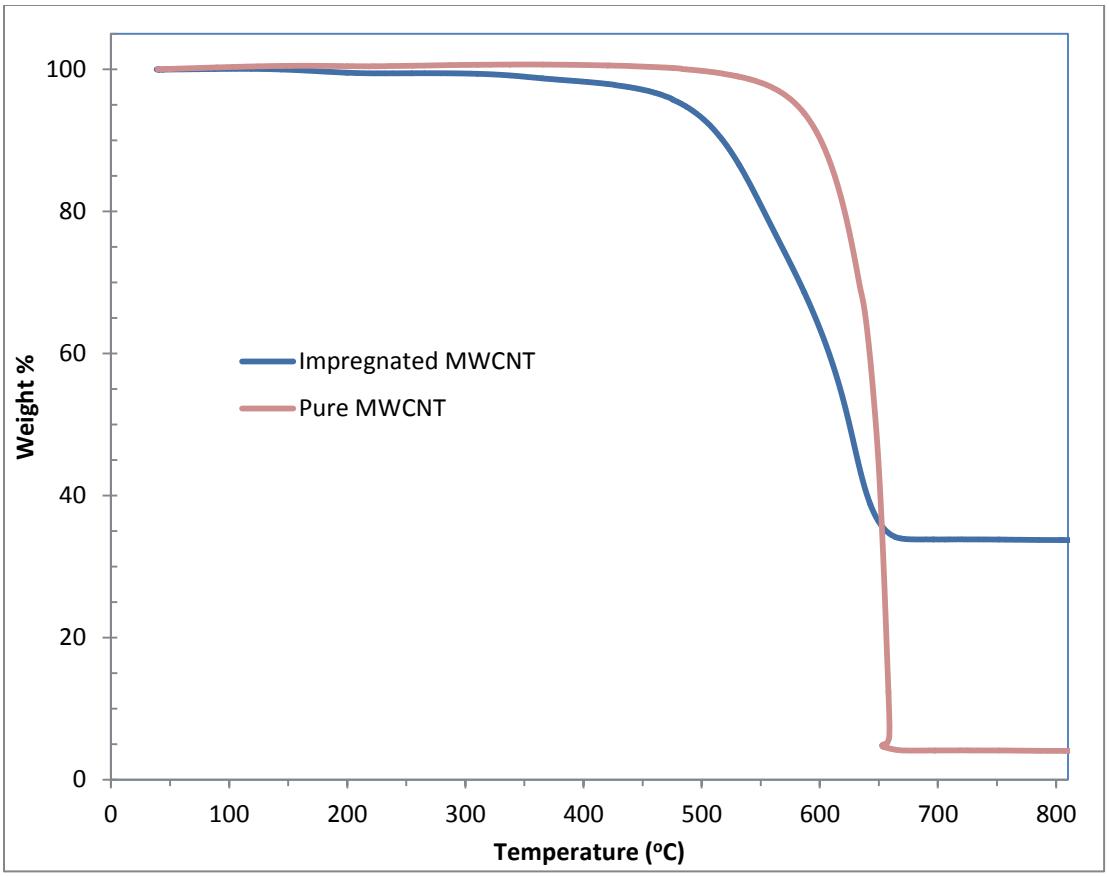

Figure 5.3: TGA analysis of impregnated and pure MWCNT

5.4 SEM & TEM analysis for Surface Morphology

SEM analysis was performed using a field emission scanning electron microscope (TESCAN MIRA 3 FEG-SEM) which provided the morphology of CNTs. SEM analysis indicated that dispersion of Al_2O_3 over CNT varied by changing reaction parameters which eventually effect impregnation process. Optimum conditions of the reaction were found after series of experiments. Up to our knowledge this type of in situ impregnation method has not been discussed previously. Conventional impregnation methods include sonication of CNT with metal/metal oxides, followed by drying and calcination process.

These type of methods do not decorate the surface of CNT efficiently and also they are time consuming (Motshekga et al., 2012).

To disperse alumina particles uniformly on the surface of CNT we proposed a novel *in situ* impregnation method. In this method, an ultrasonic atomizer was used in the reactor head to evenly-distribute feed solution in to the reactor. In this way two processes simultaneously starts; one is the formation of MWCNT and other is formation of alumina particles according to Eq. 1. Thus, alumina particles impregnate over CNT during its synthesis. This type of fine dispersion increased the surface area of feed solution particles hence chances of good impregnation increased in this technique as compared to conventional techniques.

Figure 2 indicates the images (a) to (h) of impregnated MWCNT obtained by increasing hydrogen flow rate. It was observed that higher flow rate of hydrogen gas resulted in better dispersion of alumina particles over MWCNT. Also, large bundles of MWCNT (Figure 2 b) converted into small bundles of dispersed MWCNT (Figure 2 h). Image 2a, 2c, 2d, and 2e indicate the high resolution image of MWCNT bundles and it is obvious that cloudy particles covering carbon nanotubes. These cloudy areas are actually alumina particles which are dispersed over CNT surface.

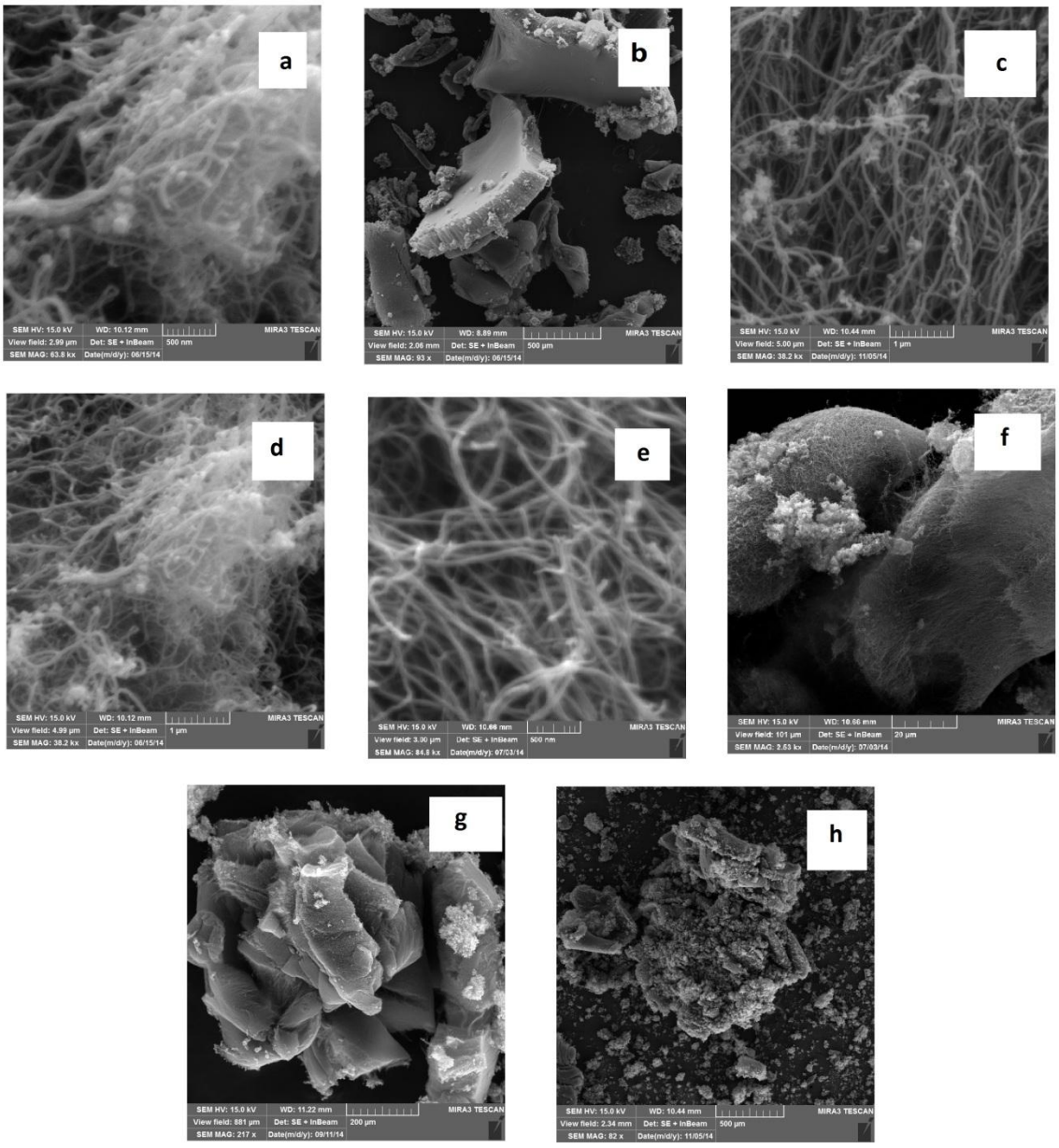

Figure 5.4: SEM images of impregnated MWCNT obtained by increasing hydrogen flow rates from (a) to (h)

Figure 3 compares the structure of pure and impregnated MWCNTs by SEM analysis. It indicates that there are no metal or impurity particles over pure MWCNT, and fine structure denotes the long carbon nanotubes (Figure 3a). Whereas, a cluster of alumina particles can be seen over surface of MWCNT in Figure 3b. This comparison proves the claim that alumina particles are dispersed over surface of MWCNT and prevents the MWCNT to form bundles. Thus by this technique high surface area MWCNT can be achieved which is not possible by sonication or other conventional techniques.

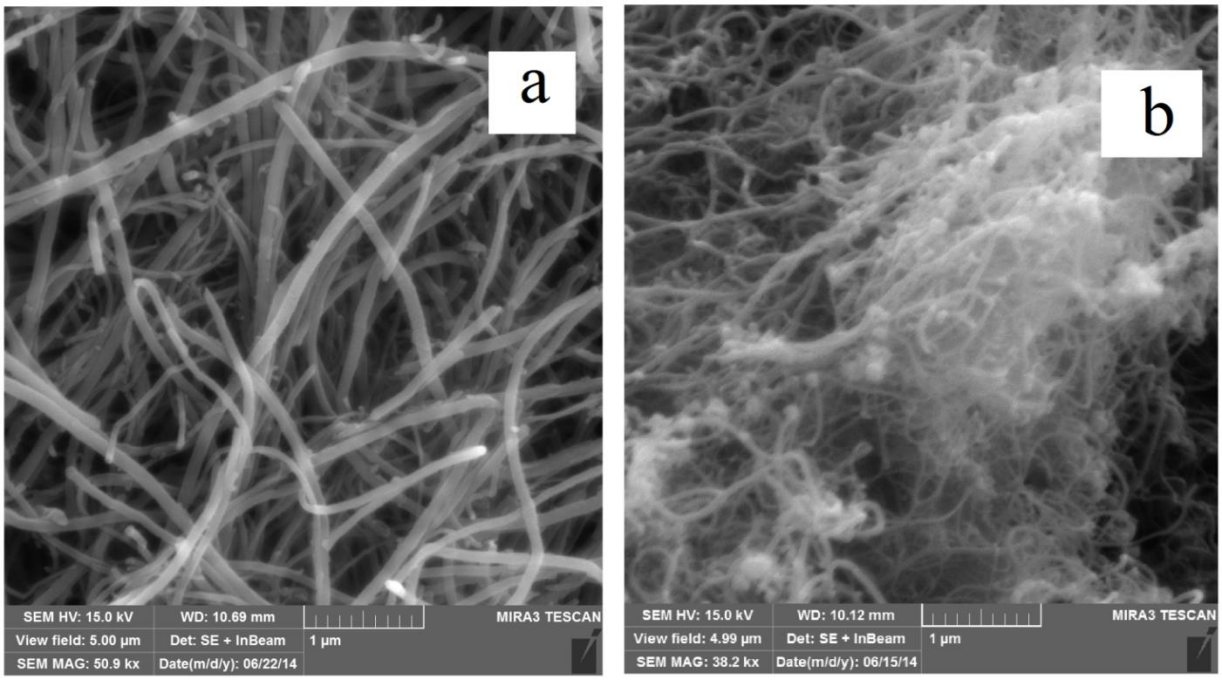

Figure 5.5: SEM images. (A) Pure MWCNT. (B) Impregnated MWCNT.

TEM analysis was performed using field emission electron microscope (JEM-2100F) which provided information about the walls and inside structure of MWCNT,and pattern of dispersion of alumina particles. TEM analysis revealed that alumina particles were not present inside the MWCNT as hollow structure of tube is visible (Figure 5). Further, the alumina particles synthesized during the reaction used to cover surface area of MWCNT. In this way a large number of active sites of metal oxide can be produced on molecular level which was not possible before. Arrows in Figure 5 indicates the beads type spherical structure of alumina on molecular scale.

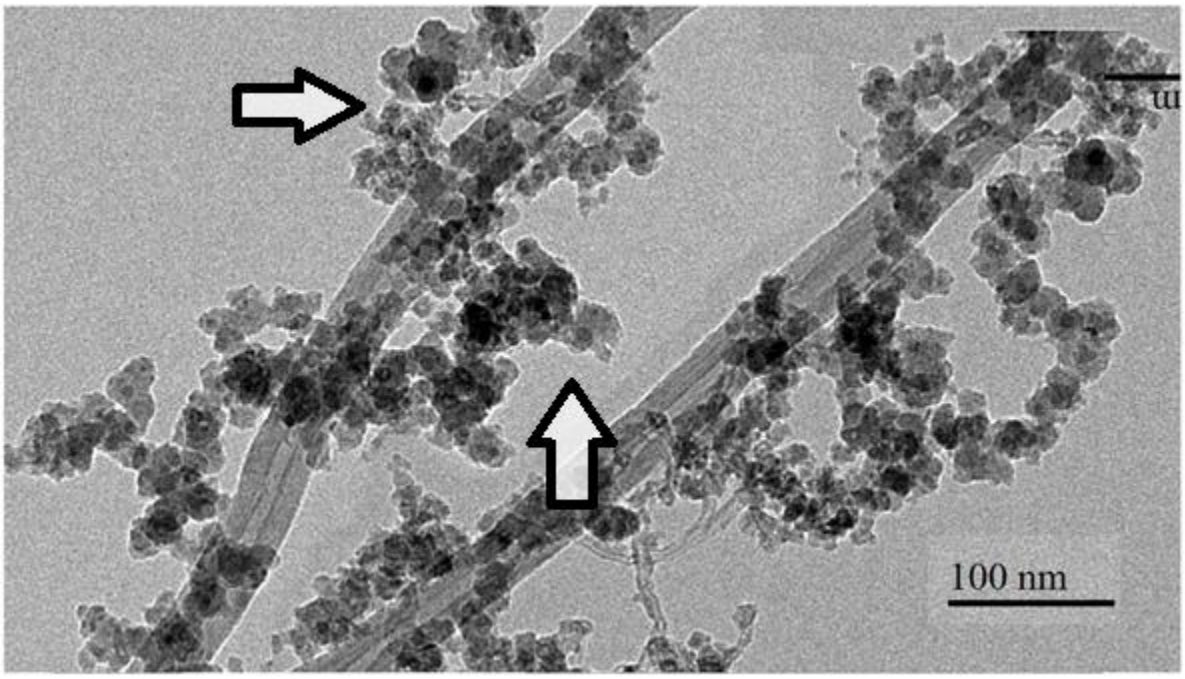

Figure 5.6: TEM images impregnated MWCNT

5.5 BET Analysis for Surface Area

Surface areas of pure MWCNT and alumina impregnated MWCNT were measured by using Brunauer-Emmett-Teller (BET) analysis. The BET theory targets the phenomenon of physical adsorption and desorption of gas molecules on a solid surface. BET analysis was made by micropore analyzer (Quantachrome, Autosorb IQM0000-4) which calculates the exact specific surface area of materials by comparing adsorption of Nitrogen adsorption at 77 K against relative pressure by using complete automated analyzer. Pure and impregnated MWCNTs were analyzed by BET technique. Result indicated that surface area of pure MWCNT was 100 m^2/g, whereas that of impregnated MWCNT was 820 m^2/g. This very high surface area of impregnated MWCNT has resulted due to evenly distribution of aluminum oxide over MWCNT surface.

CHAPTER 6

CONCLUSIONS AND RECOMMENDATIONS

6.1 Conclusions

- Full and even dispersion of catalytic solution was achieved by using a new technology of ultrasonic atomization head in IVCVD reactor.
- Maximum yield of 10 grams was achieved for one hour operation.
- More than 96 percent pure MWCNT obtained without any treatment.
- Alignment of CNT bundles can be altered as required. Flexibility in the design of the reactor makes it possible to increase the yield. The diameter, length and number of tubes of CNT can be tailored by changing reaction-temperature and H_2 flow-rate.
- Specific surface area of MWCNT was 75-90 m^2/g.
- High aspect ratio CNT was obtained at 800 ^oC and 850 ^oC by using Ferrocene in p-Xylene. Flow rate ratio of H_2 to Ar was kept constant at 3:1 respectively.
- CNT wafers were separated from quartz tube and analyzed by SEM to find length and diameter of tubes. Length of flake was found to vary between ~238 µm to ~150 µm with the diameter range ~50 nm to ~ 90 nm. Pint C. et al., (2008) (Pint et al., 2008) explains this phenomenon of formation of flying carpet flakes. According to his study Fe_2O_3 produces metallic iron in the reducing environment, such as of H_2, which is responsible for flake formation. In our work we used

FCN; for Fe catalyst particles, which is more receptive to reduction under presence of H_2.

- We obtained very high aspect ratio (l/d) CNT flakes at various point on the quartz tube which varies from 4,000 to 12,000, Figure 6.1 (a) and (b).
- Thus to utilize the effect of reducing agent, we used only H_2 at high flow rate without any carrier gas which was used in all previous experiments. In this way H_2 behaved like a reducing agent as well as self-carrier gas. CNT obtained showed larger flakes of CNT were formed that were varying up-to few millimeters length. One of the flakes that formed under pure reducing environment can be seen in Figure 6.1 (c).
- It was observed that highest yield up to 10 g/h was formed in the presence of only H_2.

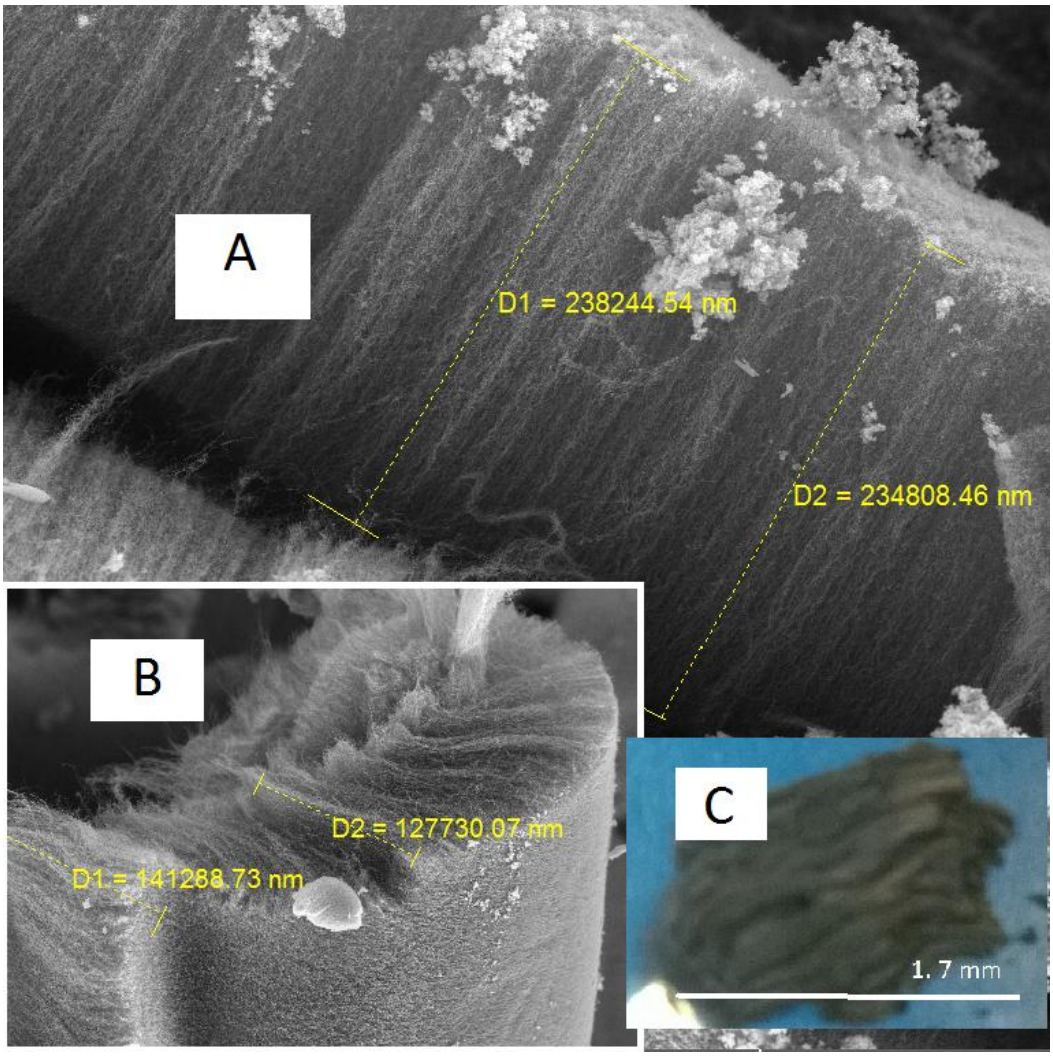

Figure 6.1. High aspect ratio MWCNT synthesized at A) H_2 and Ar flow rates 3 and 1 L/m respectively, temperature 800 ^oC, feed injection rate 90 mL/h, B) H_2 and Ar flow rates 3 and 1 L/m respectively, temperature 850 ^oC, feed injection rate 90 mL/h, C) H_2 flow rate 4 L/m and temperature 850 ^oC

- XRD characteristic peaks proved the presence of Al_2O_3 in the MWCNT sample. This means target of impregnation had been achieved.

- TEM images showed that beads of Al2O3 particles covered the MWCNT.

- BET analysis indicated that very high surface area of 820 m^2/g of MWCNT was achieved due to impregnation of alumina. By following the same route, pure MWCNT yielded 100 m^2/g of surface area.

- Single step in situ impregnated MWCNT was produced.

6.2 Recommendations

1. Effect of different ratios of catalyst to precursor can be studied.
2. The reactor can be used on a pilot plant scale as a semi-continues reactor for more than 3 hours and to study all the parameters that has been studied.
3. Behavior of different higher hydrocarbons can be studied and yield can be optimized.
4. Different ratios of aluminum isopropoxide can be used to study impregnation method in more details.
5. After complete literature review, other metallic salts can be injected into the reactor which may produce their respective metal oxides and impregnate on MWCNT.
6. Application of synthesized multiwall carbon nanotube and 1 % aluminum impregnated multiwall carbon nanotubes in removal of various heavy metals and aromatic compounds.
7. As home-synthesized MWCNT and IM-CNT showed better thermal properties than that of commercial, so it can be used as a nano-fluid in heat exchangers.

Reference

Ajayan, P. M. (1999). Nanotubes from Carbon. *Chemical Reviews*, *99*(7), 1787–1800.

Al-Hakami, S. M., Khalil, A. B., Laoui, T., & Atieh, M. A. (2013). Fast disinfection of escherichia coli bacteria using carbon nanotubes interaction with microwave radiation. *Bioinorganic Chemistry and Applications*, *2013*, 1–10. doi:10.1155/2013/458943

Al-Khaldi, F. A., Abu-Sharkh, B., Abulkibash, A. M., & Atieh, M. A. (2013). Cadmium removal by activated carbon, carbon nanotubes, carbon nanofibers, and carbon fly ash: a comparative study. *Desalination and Water Treatment*, (October), 1–13. doi:10.1080/19443994.2013.847805

Amr, I. T., Al-Amer, A., Selvin, T. P., Al-Harthi, M., Girei, S. A., Sougrat, R., & Atieh, M. A. (2011). Effect of acid treated carbon nanotubes on mechanical, rheological and thermal properties of polystyrene nanocomposites. *Composites Part B: Engineering*, *42*(6), 1554–1561. doi:10.1016/j.compositesb.2011.04.013

Andrews, R., Jacques, D., Qian, D., & Rantell, T. (2002). Multiwall Carbon Nanotubes: Synthesis and Application. *Accounts of Chemical Research*, *35*(12), 1008–1017. doi:10.1021/ar010151m

Andrews, R., Jacques, D., Rao, A. M., Derbyshire, F., Qian, D., Fan, X., … Chen, J. (1999). Continuous production of aligned carbon nanotubes: a step closer to commercial realization. *Chemical Physics Letters*, *303*(5-6), 467–474. doi:10.1016/S0009-2614(99)00282-1

Atieh, M. a. (2011). Effect of Functionalize Carbon Nanotubes with Amine Functional Group on the Mechanical and Thermal Properties of Styrene Butadiene Rubber. *Journal of Thermoplastic Composite Materials*, *24*(5), 613–624. doi:10.1177/0892705710397456

Atieh, M. A., Bakather, O. Y., Tawabini, B. S., Bukhari, A. A., Khaled, M., Alharthi, M., … Abuilaiwi, F. A. (2010). Removal of Chromium (III) from Water by Using Modified and Nonmodified Carbon Nanotubes. *Journal of Nanomaterials*, *2010*, 1–9. doi:10.1155/2010/232378

Balogh, Z., Halasi, G., Korbély, B., & Hernadi, K. (2008). CVD-synthesis of multiwall carbon nanotubes over potassium-doped supported catalysts. *Applied Catalysis A: General*, *344*(1-2), 191–197. doi:10.1016/j.apcata.2008.04.019

Barreiro, A., Selbmann, D., Pichler, T., Biedermann, K., Gemming, T., Rümmeli, M. H., … Büchner, B. (2005). On the effects of solution and reaction parameters for the

aerosol-assisted CVD growth of long carbon nanotubes. *Applied Physics A*, *82*(4), 719–725. doi:10.1007/s00339-005-3436-5

Bethune, D. S., Klang, C. H., de Vries, M. S., Gorman, G., Savoy, R., Vazquez, J., & Beyers, R. (1993). Cobalt-catalysed growth of carbon nanotubes with single-atomic-layer walls. *Nature*, *363*(6430), 605–607. doi:10.1038/363605a0

Bom, D., Andrews, R., Jacques, D., Anthony, J., Chen, B., Meier, M. S., & Selegue, J. P. (2002). Thermogravimetric Analysis of the Oxidation of Multiwalled Carbon Nanotubes: Evidence for the Role of Defect Sites in Carbon Nanotube Chemistry. *Nano Letters*, *2*(6), 615–619. doi:10.1021/nl020297u

Bower, C., Zhu, W., Jin, S., & Zhou, O. (2000). Plasma-induced alignment of carbon nanotubes. *Applied Physics Letters*, *77*(6), 830. doi:10.1063/1.1306658

Cassell, A. M., Raymakers, J. a., Kong, J., & Dai, H. (1999). Large Scale CVD Synthesis of Single-Walled Carbon Nanotubes. *The Journal of Physical Chemistry B*, *103*(31), 6484–6492. doi:10.1021/jp990957s

Chen, W.-X., Lee, J. Y., & Liu, Z. (2004). Preparation of Pt and PtRu nanoparticles supported on carbon nanotubes by microwave-assisted heating polyol process. *Materials Letters*, *58*(25), 3166–3169. doi:10.1016/j.matlet.2004.06.008

Collins, P. G., & Avouris, P. (2000). Nanotubes for Electronics. *Scientific American*, *283*(6), 62–69. doi:10.1038/scientificamerican1200-62

Corrias, M., Caussat, B., Ayral, A., Durand, J., Kihn, Y., Kalck, P., & Serp, P. (2003). Carbon nanotubes produced by fluidized bed catalytic CVD: first approach of the process. *Chemical Engineering Science*, *58*(19), 4475–4482. doi:10.1016/S0009-2509(03)00265-3

Craddock, J. D., & Weisenberger, M. C. (2014). Harvesting of large, substrate-free sheets of vertically aligned multiwall carbon nanotube arrays. *Carbon*, *81*, 839–841. doi:10.1016/j.carbon.2014.09.039

De Volder, M. F. L., Tawfick, S. H., Baughman, R. H., & Hart, a J. (2013). Carbon nanotubes: present and future commercial applications. *Science (New York, N.Y.)*, *339*(6119), 535–9. doi:10.1126/science.1222453

Dell'Acqua-Bellavitis, L. M., Ballard, J. D., Ajayan, P. M., & Siegel, R. W. (2004). Kinetics for the Synthesis Reaction of Aligned Carbon Nanotubes: A Study Based on in situ Diffractography. *Nano Letters*, *4*(9), 1613–1620. doi:10.1021/nl0492335

Dresselhaus, M. S. (1998). Nanotechnology: New tricks with nanotubes, *391*(6662), 19–20. doi:10.1038/34036

Durães, L., Costa, B. F. O., Santos, R., Correia, A., Campos, J., & Portugal, A. (2007). Fe2O3/aluminum thermite reaction intermediate and final products characterization. *Materials Science and Engineering A*, *465*(1-2), 199–210. doi:10.1016/j.msea.2007.03.063

Ebbesen, T. W., & Ajayan, P. M. (1992). Large-scale synthesis of carbon nanotubes. *Nature*, *358*(6383), 220–222. doi:10.1038/358220a0

Endo, M., Hayashi, T., Kim, Y. A., Terrones, M., & Dresselhaus, M. S. (2004). Applications of carbon nanotubes in the twenty-first century. *Philosophical Transactions. Series A, Mathematical, Physical, and Engineering Sciences*, *362*(1823), 2223–38. doi:10.1098/rsta.2004.1437

Girei, S. a., Thomas, S. P., Atieh, M. a., Mezghani, K., De, S. K., Bandyopadhyay, S., & Al-Juhani, A. (2012). Effect of -COOH Functionalized Carbon Nanotubes on Mechanical, Dynamic Mechanical and Thermal Properties of Polypropylene Nanocomposites. *Journal of Thermoplastic Composite Materials*, *25*(3), 333–350. doi:10.1177/0892705711406159

Golnabi, H. (2012). Carbon nanotube research developments in terms of published papers and patents, synthesis and production. *Scientia Iranica*, *19*(6), 2012–2022. doi:10.1016/j.scient.2012.10.036

Han, W.-Q., & Zettl, A. (2003). Coating Single-Walled Carbon Nanotubes with Tin Oxide. *Nano Letters*, *3*(5), 681–683. doi:10.1021/nl034142d

Hongo, H., Yudasaka, M., Ichihashi, T., Nihey, F., & Iijima, S. (2002). Chemical vapor deposition of single-wall carbon nanotubes on iron-film-coated sapphire substrates. *Chemical Physics Letters*, *361*(3-4), 349–354. doi:10.1016/S0009-2614(02)00963-6

Hull, R. V., Li, L., Xing, Y., & Chusuei, C. C. (2006). Pt Nanoparticle Binding on Functionalized Multiwalled Carbon Nanotubes. *Chemistry of Materials*, *18*(7), 1780–1788. doi:10.1021/cm0518978

Ihsanullah, Al-Khaldi, F. A., Abu-Sharkh, B., Abulkibash, A. M., Qureshi, M. I., Laoui, T., & Atieh, M. A. (2015). Effect of acid modification on adsorption of hexavalent chromium (Cr(VI)) from aqueous solution by activated carbon and carbon nanotubes. *Desalination and Water Treatment*, (March), 1–13. doi:10.1080/19443994.2015.1021847

Iijima, S. (1991). Helical microtubules of graphitic carbon. Retrieved November 24, 2014, from http://www.nature.com/physics/looking-back/iijima/index.html

Ikuno, T., Ryu, J.-T., Oyama, T., Ohkura, S., Baek, Y.-G., Honda, S., … Oura, K. (2002). Characterization of low temperature growth carbon nanofibers synthesized by using

plasma enhanced chemical vapor deposition. *Vacuum*, *66*(3-4), 341–345. doi:10.1016/S0042-207X(02)00141-0

Ikuno, T., Yamamoto, T., Kamizono, M., Takahashi, S., Furuta, H., Honda, S., … Oura, K. (2002). Large field emission from carbon nanotubes grown on patterned catalyst thin film by thermal chemical vapor deposition. *Physica B: Condensed Matter*, *323*(1-4), 171–173. doi:10.1016/S0921-4526(02)00891-8

Jeong, G.-H., Olofsson, N., Falk, L. K. L., & Campbell, E. E. B. (2009). Effect of catalyst pattern geometry on the growth of vertically aligned carbon nanotube arrays. *Carbon*, *47*(3), 696–704. doi:10.1016/j.carbon.2008.11.003

Jin, C., Park, J., Huh, Y., & Yong, J. (2001). Temperature effect on the growth of carbon nanotubes using thermal chemical vapor deposition. *Chemical Physics Letters*, *343*(July), 33–38.

José-Yacamán, M., Miki-Yoshida, M., Rendón, L., & Santiesteban, J. G. (1993). Catalytic growth of carbon microtubules with fullerene structure. *Applied Physics Letters*, *62*(2), 202. doi:10.1063/1.109315

Journet, C., & Bernier, P. (1998). Production of carbon nanotubes. *Applied Physics A: Materials Science & Processing*, *67*(1), 1–9. doi:10.1007/s003390050731

Jung, S.-H., Kim, M.-R., Jeong, S.-H., Kim, S.-U., Lee, O.-J., Lee, K.-H., … Park, C.-K. (2003). High-yield synthesis of multi-walled carbon nanotubes by arc discharge in liquid nitrogen. *Applied Physics A: Materials Science & Processing*, *76*(2), 285–286. doi:10.1007/s00339-002-1718-8

Kiang, C.-H., Goddard, W. A., Beyers, R., & Bethune, D. S. (1995). Carbon nanotubes with single-layer walls. *Carbon*, *33*(7), 903–914. doi:10.1016/0008-6223(95)00019-A

Kim, N. S., Lee, Y. T., Park, J., Han, J. B., Choi, Y. S., Choi, S. Y., … Lee, G. H. (2003). Vertically Aligned Carbon Nanotubes Grown by Pyrolysis of Iron, Cobalt, and Nickel Phthalocyanines. *The Journal of Physical Chemistry B*, *107*(35), 9249–9255. doi:10.1021/jp034895o

Kong, J., Soh, H. T., Cassell, A. M., Quate, C. F., & Dai, H. (1998). Synthesis of individual single-walled carbon nanotubes on patterned silicon wafers, *395*(6705), 878–881. doi:10.1038/27632

Koprinarov, N., Konstantinova, M., Ruskov, T., & Spirov, I. (2007). Ferromagnetic Nanomaterials Obtained by Thermal Decomposition of Ferrocene in a Closed Chamber. *Phys*, *34*, 17–32.

Kunadian, I., Andrews, R., Qian, D., & Pinar Mengüç, M. (2009). Growth kinetics of MWCNTs synthesized by a continuous-feed CVD method. *Carbon*, *47*(2), 384–395. doi:10.1016/j.carbon.2008.10.022

Küttel, O. M., Groening, O., Emmenegger, C., & Schlapbach, L. (1998). Electron field emission from phase pure nanotube films grown in a methane/hydrogen plasma. *Applied Physics Letters*, *73*(15), 2113. doi:10.1063/1.122395

Lee, C. J., Park, J., & Yu, J. A. (2002). Catalyst effect on carbon nanotubes synthesized by thermal chemical vapor deposition. *Chemical Physics Letters*, *360*(July), 250–255.

Lee, S. W., Kim, B.-S., Chen, S., Shao-Horn, Y., & Hammond, P. T. (2009). Layer-by-layer assembly of all carbon nanotube ultrathin films for electrochemical applications. *Journal of the American Chemical Society*, *131*(2), 671–9. doi:10.1021/ja807059k

Li, J., & Zhang, Y. (2006). Large-scale aligned carbon nanotubes films. *Physica E: Low-Dimensional Systems and Nanostructures*, *33*(1), 235–239. doi:10.1016/j.physe.2006.02.034

Li, Y., Cui, R., Ding, L., Liu, Y., Zhou, W., Zhang, Y., … Liu, J. (2010). How catalysts affect the growth of single-walled carbon nanotubes on substrates. *Advanced Materials (Deerfield Beach, Fla.)*, *22*(13), 1508–15. doi:10.1002/adma.200904366

Li, Y.-L., Zhang, L.-H., Zhong, X.-H., & Windle, A. H. (2007). Synthesis of high purity single-walled carbon nanotubes from ethanol by catalytic gas flow CVD reactions. *Nanotechnology*, *18*(22), 225604. doi:10.1088/0957-4484/18/22/225604

Mamalis, A. ., Vogtländer, L. O. ., & Markopoulos, A. (2004). Nanotechnology and nanostructured materials: trends in carbon nanotubes. *Precision Engineering*, *28*(1), 16–30. doi:10.1016/j.precisioneng.2002.11.002

Mao, C., Solis, D. J., Reiss, B. D., Kottmann, S. T., Sweeney, R. Y., Hayhurst, A., … Belcher, A. M. (2004). Virus-based toolkit for the directed synthesis of magnetic and semiconducting nanowires. *Science (New York, N.Y.)*, *303*(5655), 213–7. doi:10.1126/science.1092740

Mauron, P., Emmenegger, C., Sudan, P., Wenger, P., Rentsch, S., & Züttel, A. (2003). Fluidised-bed CVD synthesis of carbon nanotubes on Fe2O3/MgO. *Diamond and Related Materials*, *12*(3-7), 780–785. doi:10.1016/S0925-9635(02)00337-0

Mekasuwandumrong, O., Kominami, H., Praserthdam, P., & Inoue, M. (2004). Synthesis of Thermally Stable x -Alumina by Thermal Decomposition of Aluminum Isopropoxide in Toluene. *Journal of the American Ceramic Society*, *87*(8), 1543–1549.

Merkulov, V. I., Melechko, A. V., Guillorn, M. A., Lowndes, D. H., & Simpson, M. L. (2002). Growth rate of plasma-synthesized vertically aligned carbon nanofibers. *Chemical Physics Letters*, *361*(5-6), 492–498. doi:10.1016/S0009-2614(02)01016-3

Messina, G., Modafferi, V., Santangelo, S., Tripodi, P., Donato, M. G., Lanza, M., … Pistone, A. (2008). Large-scale production of high-quality multi-walled carbon nanotubes: Role of precursor gas and of Fe-catalyst support. *Diamond and Related Materials*, *17*(7-10), 1482–1488. doi:10.1016/j.diamond.2008.01.060

Mezghani, K., Farooqui, M., Furquan, S., & Atieh, M. (2011). Influence of carbon nanotube (CNT) on the mechanical properties of LLDPE/CNT nanocomposite fibers. *Materials Letters*, *65*(23-24), 3633–3635. doi:10.1016/j.matlet.2011.08.002

Morançais, A., Caussat, B., Kihn, Y., Kalck, P., Plee, D., Gaillard, P., … Serp, P. (2007). A parametric study of the large scale production of multi-walled carbon nanotubes by fluidized bed catalytic chemical vapor deposition. *Carbon*, *45*(3), 624–635. doi:10.1016/j.carbon.2006.10.009

Motshekga, S. C., Pillai, S. K., Sinha Ray, S., Jalama, K., & Krause, R. W. M. (2012). Recent Trends in the Microwave-Assisted Synthesis of Metal Oxide Nanoparticles Supported on Carbon Nanotubes and Their Applications. *Journal of Nanomaterials*, *2012*, 1–15. doi:10.1155/2012/691503

Muataz, A. A., Ahmadun, F., Guan, C., Mahdi, E., & A, R. (2006). Effect of reaction temperature on the production of carbon nanotubes. *Nano*, *01*(03), 251–257. doi:10.1142/S1793292006000288

Mubarak, N. M., Abdullah, E. C., Jayakumar, N. S., & Sahu, J. N. (2014). An overview on methods for the production of carbon nanotubes. *Journal of Industrial and Engineering Chemistry*, *20*(4), 1186–1197. doi:10.1016/j.jiec.2013.09.001

Nikolaev, P., Bronikowski, M. J., Bradley, R. K., Rohmund, F., Colbert, D. T., Smith, K. ., & Smalley, R. E. (1999). Gas-phase catalytic growth of single-walled carbon nanotubes from carbon monoxide. *Chemical Physics Letters*, *313*(1-2), 91–97. doi:10.1016/S0009-2614(99)01029-5

Nuchter, M., Ondruschka, B., Bonrath, W., & Gum, A. (2004). Microwave assisted synthesis -- a critical technology overview. *Green Chemistry*, *6*(3), 128. doi:10.1039/b310502d

Öncel, Ç., & Yürüm, Y. (2006). Carbon Nanotube Synthesis via the Catalytic CVD Method: A Review on the Effect of Reaction Parameters. *Fullerenes, Nanotubes and Carbon Nanostructures*, *14*(1), 17–37. doi:10.1080/15363830500538441

Paradise, M., & Goswami, T. (2007). Carbon nanotubes – Production and industrial applications. *Materials & Design*, *28*(5), 1477–1489. doi:10.1016/j.matdes.2006.03.008

Perez-Cabero, M., Rodriguez-Ramos, I., & Guerrero-Ruiz, A. (2003). Characterization of carbon nanotubes and carbon nanofibers prepared by catalytic decomposition of acetylene in a fluidized bed reactor. *Journal of Catalysis*, *215*(2), 305–316. doi:10.1016/S0021-9517(03)00026-5

Pierson, H. O. (1996). *Handbook of Refractory Carbides & Nitrides: Properties, Characteristics, Processing and Apps.* William Andrew. Retrieved from http://books.google.com/books?hl=en&lr=&id=K_K7q3jaqXEC&pgis=1

Pierson, H. O. (1999). *Handbook of Chemical Vapor Deposition, 2nd Edition: Principles, Technology and Applications*. William Andrew. Retrieved from http://books.google.com/books?id=GIsa4vuJgcUC&pgis=1

Pint, C. L., Pheasant, S. T., Pasquali, M., Coulter, K. E., Schmidt, H. K., & Hauge, R. H. (2008). Synthesis of high aspect-ratio carbon nanotube "flying carpets" from nanostructured flake substrates. *Nano Letters*, *8*(7), 1879–83. doi:10.1021/nl0804295

Rashidi, A., Lotfi, R., Fakhrmosavi, E., & Zare, M. (2011). Production of single-walled carbon nanotubes from methane over Co-Mo / MgO nanocatalyst : A comparative study of fixed and fluidized bed reactors. *Journal of Natural Gas Chemistry*, *20*(4), 372–376. doi:10.1016/S1003-9953(10)60208-3

Reddy, K. R., Lee, K.-P., Gopalan, A. I., Kim, M. S., Showkat, A. M., & Nho, Y. C. (2006). Synthesis of metal (Fe or Pd)/alloy (Fe–Pd)-nanoparticles-embedded multiwall carbon nanotube/sulfonated polyaniline composites by γ irradiation. *Journal of Polymer Science Part A: Polymer Chemistry*, *44*(10), 3355–3364. doi:10.1002/pola.21451

Ren, Zhifeng ; Huang, Zhongping ; J Wang, ui H.; Wang, D. . (2005, March 8). Free-standing and aligned carbon nanotubes and synthesis thereof. Retrieved from http://www.google.com/patents/US6863942

Richter, H., Hernadi, K., Caudano, R., Fonseca, a., Migeon, H. N., Nagy, J. B., … Van Tiggelen, P. J. (1996). Formation of nanotubes in low pressure hydrocarbon flames. *Carbon*, *34*(3), 427–429. doi:10.1016/0008-6223(96)87612-3

Rinaldi, A., Abdullah, N., Ali, M., Furche, A., Hamid, S. B. A., Su, D. S., & Schlögl, R. (2009). Controlling the yield and structure of carbon nanofibers grown on a nickel/activated carbon catalyst. *Carbon*, *47*(13), 3023–3033. doi:10.1016/j.carbon.2009.06.056

Roco, M. C., Mirkin, C. A., & Hersam, M. C. (2011). Nanotechnology research directions for societal needs in 2020: summary of international study. *Journal of Nanoparticle Research, 13*(3), 897–919. doi:10.1007/s11051-011-0275-5

Satishkumar, B. C., Govindaraj, A., & Rao, C. N. R. (1999). Bundles of aligned carbon nanotubes obtained by the pyrolysis of ferrocene–hydrocarbon mixtures: role of the metal nanoparticles produced in situ. *Chemical Physics Letters*, *307*(3-4), 158–162. doi:10.1016/S0009-2614(99)00521-7

Satishkumar, B. C., Thomas, P. J., Govindaraj, A., & Rao, C. N. R. (2000). Y-junction carbon nanotubes. *Applied Physics Letters*, *77*(16), 2530. doi:10.1063/1.1319185

Schadler, L. S., Giannaris, S. C., & Ajayan, P. M. (1998). Load transfer in carbon nanotube epoxy composites. *Applied Physics Letters*, *73*(26), 3842. doi:10.1063/1.122911

Schujman, S. B., Vajtai, R., Biswas, S., Dewhirst, B., Schowalter, L. J., & Ajayan, P. (2002). Electrical behavior of isolated multiwall carbon nanotubes characterized by scanning surface potential microscopy. *Applied Physics Letters*, *81*(3), 541. doi:10.1063/1.1490401

Shaikjee, A., & Coville, N. J. (2012). The role of the hydrocarbon source on the growth of carbon materials. *Carbon*, *50*(10), 3376–3398. doi:10.1016/j.carbon.2012.03.024

Singh, C., Shaffer, M. S. ., & Windle, A. H. (2002). Production of controlled architectures of aligned carbon nanotubes by an injection chemical vapour deposition method. *Carbon*, *41*(2), 359–368. doi:10.1016/S0008-6223(02)00314-7

Sinnott, S. B., Andrews, R., Qian, D., Rao, A. M., Mao, Z., Dickey, E. C., & Derbyshire, F. (1999). Model of carbon nanotube growth through chemical vapor deposition. *Chemical Physics Letters*, *315*(1-2), 25–30. doi:10.1016/S0009-2614(99)01216-6

Tapasztó, L., Kertész, K., Vértesy, Z., Horváth, Z. E., Koós, A. a., Osváth, Z., … Biró, L. P. (2005). Diameter and morphology dependence on experimental conditions of carbon nanotube arrays grown by spray pyrolysis. *Carbon*, *43*(5), 970–977. doi:10.1016/j.carbon.2004.11.048

Tawabini, B., Al-Khaldi, S., Atieh, M., & Khaled, M. (2010). Removal of mercury from water by multi-walled carbon nanotubes. *Water Science and Technology*, *61*(3), 591–598. doi:10.2166/wst.2010.897

Vahlas, C., Caussat, B., Serp, P., & Angelopoulos, G. N. (2006). Principles and applications of CVD powder technology. *Materials Science and Engineering: R: Reports*, *53*(1-2), 1–72. doi:10.1016/j.mser.2006.05.001

Varadan, V. K., & Xie, J. (2002). Large-scale synthesis of multi-walled carbon nanotubes by microwave CVD. *Smart Materials and Structures*, *11*(4), 610–616. doi:10.1088/0964-1726/11/4/318

Venegoni, D., Serp, P., Feurer, R., Kihn, Y., Vahlas, C., & Kalck, P. (2002). Parametric study for the growth of carbon nanotubes by catalytic chemical vapor deposition in a fluidized bed reactor. *Carbon*, *40*, 1799–1807.

Venegonia, Ph; R, Serp; R, Feurer; Y, K. (2002). Parametric study for the growth of carbon nanotubes by catalytic chemical vapor deposition in a fluidized bed reactor. *Carbon*, *4*, 1799–1807.

Wagner, H. D., Lourie, O., Feldman, Y., & Tenne, R. (1998). Stress-induced fragmentation of multiwall carbon nanotubes in a polymer matrix. *Applied Physics Letters*, *72*(2), 188. doi:10.1063/1.120680

Wang, S., Jiang, S. P., White, T. J., Guo, J., & Wang, X. (2009). Electrocatalytic Activity and Interconnectivity of Pt Nanoparticles on Multiwalled Carbon Nanotubes for Fuel Cells. *The Journal of Physical Chemistry C*, *113*(43), 18935–18945. doi:10.1021/jp906923z

Wang, X. Q., Li, L., Chu, N. J., Liu, Y. P., Jin, H. X., & Ge, H. L. (2009). Lamellar Fe/Al2O3 catalyst for high-yield production of multi-walled carbon nanotubes bundles. *Materials Research Bulletin*, *44*(2), 422–425. doi:10.1016/j.materresbull.2008.04.022

Wang, Y., Wei, F., Gu, G., & Yu, H. (2002). Agglomerated carbon nanotubes and its mass production in a fluidized-bed reactor. *Physica B: Condensed Matter*, *323*(1-4), 327–329. doi:10.1016/S0921-4526(02)01041-4

Wang, Y., Wei, F., Luo, G., Yu, H., & Gu, G. (2002). The large-scale production of carbon nanotubes in a nano-agglomerate fluidized-bed reactor. *Chemical Physics Letters*, *364*(5-6), 568–572. doi:10.1016/S0009-2614(02)01384-2

Weizhong, Q., Tang, L., Zhanwen, W., Fei, W., Zhifei, L., Guohua, L., & Yongdan, L. (2004). Production of hydrogen and carbon nanotubes from methane decomposition in a two-stage fluidized bed reactor. *Applied Catalysis A: General*, *260*(2), 223–228. doi:10.1016/j.apcata.2003.10.018

Wu, B., Hu, D., Kuang, Y., Liu, B., Zhang, X., & Chen, J. (2009). Functionalization of carbon nanotubes by an ionic-liquid polymer: dispersion of Pt and PtRu nanoparticles on carbon nanotubes and their electrocatalytic oxidation of methanol. *Angewandte Chemie (International Ed. in English)*, *48*(26), 4751–4. doi:10.1002/anie.200900899

Xu, Q.-C., Lin, J.-D., Li, J., Fu, X.-Z., Liang, Y., & Liao, D.-W. (2007). Microwave-assisted synthesis of MgO–CNTs supported ruthenium catalysts for ammonia synthesis. *Catalysis Communications*, *8*(12), 1881–1885. doi:10.1016/j.catcom.2007.03.002

Xue, B., Chen, P., Hong, Q., Lin, J., & Tan, K. L. (2001). Growth of Pd, Pt, Ag and Au nanoparticles on carbon nanotubes. *Journal of Materials Chemistry*, *11*(9), 2378–2381. doi:10.1039/b100618p

Zeino, A., Abulkibash, A., Khaled, M., & Atieh, M. (2014). Bromate Removal from Water Using Doped Iron Nanoparticles on Multiwalled Carbon Nanotubes (CNTS). *Journal of Nanomaterials*, *2014*.

Zhao, Y., Fan, L., Zhong, H., Li, Y., & Yang, S. (2007). Platinum Nanoparticle Clusters Immobilized on Multiwalled Carbon Nanotubes: Electrodeposition and Enhanced Electrocatalytic Activity for Methanol Oxidation. *Advanced Functional Materials*, *17*(9), 1537–1541. doi:10.1002/adfm.200600416

Zheng, B., Li, Y., & Liu, J. (2002). CVD synthesis and purification of single-walled carbon nanotubes on aerogel-supported catalyst. *Applied Physics A: Materials Science & Processing*, *74*(3), 345–348. doi:10.1007/s003390201275

VITAE

Fahad Ali Rabbani

engineer.rabbani@yahoo.com

Currenet address:

KFUPM Box 8288,
Dhahran 31261, Saudi Arabia

Mob: (+966) 55 741 5314

Permanent address:

House 2, Street 174, Ali Street,
College Road, Baghbanpura, Lahore,
Pakistan

Mob: (+92) 345 4174611

EDUCATION

MS in Chemical Engineering — **Jan 2013 To May 2015**

King Fahd University of Petroleum and Minerals

Saudi Arabia

B.Sc in Chemical Engineering — **Jul 2007 To Jul 2011**

The University of the Punjab, Lahore, Pakistan

ACADEMIC ACHIEVEMENTS

Recipient of **graduate research scholarship** at KFUPM for MS

Recipient of the **University Merit Scholarship** in 2009 and 2010

RESEARCH ACHIEVEMENTS

Two Patents accepted.

Two papers *(submitted)*

"*Synthesis of substrate-free aligned and tailored high aspect ratio multiwall carbon nanotubes in vertical CVD reactor by using p-Xylene and ferrocene."*

&

"In-situ and single step impregnation of aluminum di-oxide on multiwall carbon nanotubes to produce high specific surface area MWCNT in vertical CVD reactor."

SEMINARS AND WORKSHOPS

CHEMCAD Steady State Process Simulation (Basics)
CHEMCAD Heat Exchanger Design & Rating.
Energy Conservation & Sustainability.
Safety Standards for Industry
Strategic Management

ANALYTICAL SKILLS

Total organic carbon (TOC)

Gas Chromatography Flame Ionized (GC-FID)

Gas Chromatography Mass Spectrometer (GC-MS)

RESEARCH PROJECT

CNT synthesis by using Injected Vertical CVD Reactor fitted with an Ultrasonic Atomizer from p-Xylene. (MS Thesis)
Advisor Dr. Zuhair Omar Malaibari

Aug 2013 To May 2013t

ACADEMIC TRAINING

Internship at Engro Fertilizer Limited, Dharki

*Submitted a report for a mini project to find problems and possible solutions of **flow transmitters fitted at boilers**.*

ACADEMIC PROJECTS

Project on Production of 10,000 MTPY of Monomer by using Acetylene and Acetic Acid

2010 To 2011

Prepared a detail report of plant design, the piping & instrumentation diagram, the design of reactors, separation equipment, pumps and piping design including the environmental impact assessment, the HAZOP analysis and the economic evaluation of the plant

Conversion of Tap Water into Mineral Water

Jan To May 2009

Used RO membrane, de-ionization and UV treatment for removing any solids from tap water and met W.H.O. standards of drinking water by adding accurate amount of minerals.

PART TIME JOBS (MS)	Worked as an instructor to under graduate in Mass Transfer labs of Chemical Engineering Worked as a lab assistant, in the Center of Environment and Water, Research Institute

COMPUTING SKILLS	Microsoft Word *(Higher level)*	Excel *(Advanced level)*
	Outlook *(Higher level)*	Power Point *(Higher level)*
	Photoshop *(Basic level)*	Mathematica *(Basic level)*
	MATLAB *(Basic level)*	

LANGUAGES KNOWN	Proficient and fluent in English Urdu (native) and Arabic (beginner)

PERSONAL DETAILS	Father's Name:	Mr. Qais Ali Rabbani
	Date of Birth:	10 - Sep - 1989
	Marital Status:	Unmarried
	Nationality:	Pakistan
	Place of Birth:	Lahore, Pakistan